Study of discrete duality finite volume schemes for the Peaceman model

Claire Chainais-Hillairet, Stella Krell, Alexandre Mouton

Study of discrete duality finite volume schemes for the Peaceman model ☆

C. Chainais-Hillairet[a], S. Krell[b], A. Mouton[a]

[a] *Laboratoire P. Painlevé, CNRS UMR 8524, Université Lille 1, 59655 Villeneuve d'Ascq Cedex*
[b] *Laboratoire J. Dieudonné, CNRS UMR 7351, Université de Nice - Sophia Antipolis*

Abstract

In this paper, we are interested in the finite volume approximation of a system describing miscible displacement in porous media. This system is made of two coupled equations: an anisotropic diffusion equation on the pressure and a convection-diffusion-dispersion equation on the concentration of invading fluid. The anisotropic diffusion operators in both equations require a special care while discretizing by a finite volume method. We focus here on the numerical approximation by some Discrete Duality Finite Volume methods. After the presentation of the scheme, we establish some a priori estimates satisfied by the numerical solution and prove existence and uniqueness of the solution to the scheme. We show the efficiency of the schemes through numerical experiments.

Keywords:
finite volume method, porous medium

1. Introduction

1.1. Finite volume methods for diffusion operators

Finite volume methods have been extensively studied for a long time in several engineering fields. Indeed, they are well suited for the numerical approximation of conservation laws appearing for instance in fluid mechanics, petroleum engineering and many other fields. The theoretical analysis of finite volume schemes (convergence analysis, error estimates,...) began at the end of the 1980's and had a rapid expansion during the 1990's : see for instance the book by Eymard, Gallouët, Herbin [20] and all the references therein. However, if finite volume schemes were particularly competitive and popular for the approximation of hyperbolic conservation laws, they were less used for the approximation of diffusion. Indeed, the classical two-points flux approximation for diffusion operators, firstly developed and analyzed, has many drawbacks:

- its use for the Laplace operator is limited to admissible meshes (satisfying some orthogonality condition),
- its extension to anisotropic diffusion operator implies a more restrictive assumption on the meshes which makes it difficult to use,
- its extension to nonlinear diffusion operators like Leray-Lions operators is not possible because the scheme is based on a two-points approximation of normal gradients and therefore no discrete gradient is underlying.

For all these reasons, different teams began to work at the end of the 1990's on the development of new finite volume schemes for diffusion equations. Their aim was to provide some discrete reconstruction of gradients and then schemes applicable on almost general meshes and for linear anisotropic diffusion operators or nonlinear Leray-Lions operators. Let us cite for instance the Multi Points Flux Approximation schemes by Aavatsmark, Barkve, Boe and Mannseth[1, 2], the Discrete Duality Finite Volume schemes by Domelevo and Omnes [13, 5], the Mixed Finite Volume schemes

☆ This work has been supported by the ANR project VFSitCom, the GDR CNRS ACEN/MOMAS and by the project-team INRIA/SIMPAF
Email addresses: Claire.Chainais@math.univ-lille1.fr (C. Chainais-Hillairet), krell@unice.fr (S. Krell), Alexandre.Mouton@math.univ-lille1.fr (A. Mouton)

by Droniou and Eymard [17, 16], the Scheme Using Stabilization and Hybrid Interfaces by Eymard, Gallouët and Herbin [21, 22].

All these new methods have been compared in 2008 on a benchmark organized by Herbin and Hubert [24] (the comparison also included finite element methods, discontinuous Galerkin methods, mimetic finite difference methods and other finite volume methods...). The benchmark was devoted to the anisotropic diffusion equation $-\mathrm{div}\mathbb{K}\nabla u = f$ and included many different two-dimensional test cases. A three-dimensional benchmark was also organized in 2011, [23].

1.2. A system modeling miscible fluid flows in porous media

In this paper, we want to apply one of the finite volume method dedicated to anisotropic diffusion, the Discrete Duality Finite Volume method, to a two-dimensional system arising in petroleum engineering. The Peaceman model describes the single-phase miscible displacement of one fluid by another in a porous medium, in the case where the fluids are assumed incompressible and the gravity is neglected; it has been introduced in [6, 14]. The reservoir is described by a bounded domain $\Omega \subset \mathbb{R}^2$. The unknowns of the problem are p the pressure in the mixture, $\mathbf{U}$ its Darcy velocity and c the concentration of the invading fluid, which are defined on a time interval $(0, T)$. The porous medium is characterized by its porosity $\Phi(x)$ and its permeability $\mathbb{K}(x)$. We denote by $\mu(c)$ the viscosity of the fluid mixture, $\widehat{c}$ the injected concentration, q^+ and q^- the injection and the production source terms. The model writes:

$$\begin{cases} \mathrm{div}(\mathbf{U}) = q^+ - q^- & \text{in }]0,T[\times\Omega, \\ \mathbf{U} = -\dfrac{\mathbb{K}(x)}{\mu(c)}\nabla p & \text{in }]0,T[\times\Omega, \end{cases} \tag{1}$$

$$\Phi(x)\partial_t c - \mathrm{div}(\mathbb{D}(x,\mathbf{U})\nabla c - c\mathbf{U}) + q^- c = q^+\widehat{c} \quad \text{in }]0,T[\times\Omega, \tag{2}$$

where $\mathbb{D}$ is the diffusion-dispersion tensor including molecular diffusion and mechanical dispersion. It is given by

$$\mathbb{D}(x,\mathbf{U}) = \Phi(x)\Big(d_m\mathbb{I} + |\mathbf{U}|\Big(d_l\mathbb{E}(\mathbf{U}) + d_t(\mathbb{I} - \mathbb{E}(\mathbf{U}))\Big)\Big), \tag{3}$$

where $\mathbb{I}$ is the identity matrix, d_m is the molecular diffusion, d_l and d_t are the longitudinal and transverse dispersion coefficients and $\mathbb{E}(\mathbf{U}) = \left(\frac{\mathbf{U}_i\mathbf{U}_j}{|\mathbf{U}|^2}\right)_{1\le i,j\le d}$. The system (1)–(3) is supplemented with an initial condition on c and Neumann boundary conditions (the boundary $\partial\Omega$ is assumed impermeable). Due to the Neumann boundary conditions, the injection and the production source terms must satisfy a compatibility condition and the pressure is defined up to an arbitrary constant. The viscosity μ is usually determined by the following mixing rule:

$$\mu(c) = \mu(0)\Big(1 + \Big(M^{1/4} - 1\Big)c\Big)^{-4} \text{ on } [0,1], \tag{4}$$

where $M = \frac{\mu(0)}{\mu(1)}$ is the mobility ratio (we extend μ to $\mathbb{R}$ by letting $\mu = \mu(0)$ on $]-\infty, 0[$ and $\mu = \mu(1)$ on $]1, \infty[$). The porosity Φ and the permeability $\mathbb{K}$ are in general assumed to be bounded from above and from below by positive constants (or positive multiples of $\mathbb{I}$ for the tensor $\mathbb{K}$).

Many different schemes have already been proposed for the Peaceman model since the beginning of the 1980's. In [15], Douglas, Ewing and Wheeler proposed a mixed finite element method for the pressure equation (1) and a Galerkin finite element method for the concentration equation (2). Russel in [29] introduced a modified method of characteristic for the concentration equation and discretized the pressure equation by a finite element method. Then, Russel, Ewing and Wheeler combined mixed finite element method for (1) and a modified method of characteristic for (2), see [19, 18]. We also refer to the work by Jaffré and Roberts [27]. In [30, 31], Wang and his coauthors still use a mixed finite element method for the pressure equation but develop a Eulerian Lagrangian Localized Adjoint Method for the concentration equation. In all these papers, the pressure equation is approximated by a finite element scheme. Indeed, due to the anisotropy in the permeability tensor and in the diffusion-dispersion tensor, the system cannot be approached by classical finite volume methods and the development of finite volume schemes dedicated to anisotropy, as explained in the previous section, is new. Therefore the first finite volume methods for the Peaceman

model have been developed recently. A mixed finite volume method for both equations (1), (2) has been proposed by Chainais-Hillairet and Droniou and its convergence has been established [9]. In [3], Amaziane and El Ossmani use a mixed finite element method for (1) but propose a finite volume scheme written on a dual mesh for (2). In this paper, we will consider the application of the Discrete Duality Finite Volume methods (see [13, 5, 8]) to the Peaceman model.

1.3. Contents and outline of the paper

Let us first rewrite the Peaceman model under the following synthesized form, as in [9]:

$$\begin{aligned} &\operatorname{div}(\mathbf{U}) = q^+ - q^- && \text{in }]0,T[\times\Omega,\\ &\mathbf{U} = -\mathbb{A}(\cdot,c)\nabla p && \text{in }]0,T[\times\Omega,\\ &\mathbf{U}\cdot\mathbf{n} = 0 && \text{on }]0,T[\times\partial\Omega,\\ &\int_\Omega p(\cdot,x)\,dx = 0 && \text{on }]0,T[, \end{aligned} \tag{5}$$

$$\begin{aligned} &\Phi\partial_t c - \operatorname{div}(\mathbb{D}(\cdot,\mathbf{U})\nabla c) + \operatorname{div}(c\mathbf{U}) + q^-\bar{c} = q^+\widehat{c} && \text{in }]0,T[\times\Omega,\\ &\mathbb{D}(\cdot,\mathbf{U})\nabla c\cdot\mathbf{n} = 0 && \text{on }]0,T[\times\partial\Omega,\\ &c(0,\cdot) = c_0 && \text{on } \Omega. \end{aligned} \tag{6}$$

In the sequel, we assume that Ω is a convex polygonal bounded open subset of $\mathbb{R}^2$ and that $T > 0$. The assumptions on the data are the following:

$$\begin{gathered}(q^+,q^-)\in L^\infty(0,T;L^2(\Omega)) \text{ are nonnegative functions such that}\\ \int_\Omega q^+(\cdot,x)\,dx = \int_\Omega q^-(\cdot,x)\,dx \text{ a.e. on }]0,T[,\end{gathered} \tag{7}$$

$$\begin{gathered}\mathbb{A}:\Omega\times\mathbb{R}\to\mathcal{M}_2(\mathbb{R}) \text{ is a Caratheodory matrix-valued function satisfying:}\\ \exists\alpha_A>0 \text{ such that } \mathbb{A}(x,s)\boldsymbol{\xi}\cdot\boldsymbol{\xi}\geq\alpha_A|\boldsymbol{\xi}|^2 \text{ for a.e. } x\in\Omega, \text{ all } s\in\mathbb{R} \text{ and all } \boldsymbol{\xi}\in\mathbb{R}^2,\\ \exists\Lambda_A>0 \text{ such that } |\mathbb{A}(x,s)|\leq\Lambda_A \text{ for a.e. } x\in\Omega \text{ and all } s\in\mathbb{R},\end{gathered} \tag{8}$$

$$\begin{gathered}\mathbb{D}:\Omega\times\mathbb{R}^2\to\mathcal{M}_2(\mathbb{R}) \text{ is a Caratheodory matrix-valued function satisfying:}\\ \exists\alpha_D>0 \text{ s.t. } \mathbb{D}(x,\mathbf{W})\xi\cdot\xi\geq\alpha_D(1+|\mathbf{W}|)|\xi|^2 \text{ for a.e. } x\in\Omega, \text{ all } \mathbf{W}\in\mathbb{R}^2 \text{ and all } \xi\in\mathbb{R}^2,\\ \exists\Lambda_D>0 \text{ such that } |\mathbb{D}(x,\mathbf{W})|\leq\Lambda_D(1+|\mathbf{W}|) \text{ for a.e. } x\in\Omega \text{ and all } \mathbf{W}\in\mathbb{R}^2,\end{gathered} \tag{9}$$

$$\Phi\in L^\infty(\Omega) \text{ and there exists } \Phi_*>0 \text{ such that } \Phi_*\leq\Phi\leq\Phi_*^{-1} \text{ a.e. in } \Omega, \tag{10}$$

$$\widehat{c}\in L^\infty(]0,T[\times\Omega) \text{ satisfies: } 0\leq\widehat{c}\leq 1 \text{ a.e. in }]0,T[\times\Omega, \tag{11}$$

$$c_0\in L^\infty(\Omega) \text{ satisfies: } 0\leq c_0\leq 1 \text{ a.e. in } \Omega. \tag{12}$$

The DDFV schemes are devoted to the numerical approximation of anisotropic diffusion operators as we have in (5) and (6). They are based on two fundamental ideas: integration of the equations on a primal and a dual meshes, as suggested by Hermeline [25, 26], reconstruction of discrete gradients on a diamond mesh, as in the work by Coudière, Vila and Villedieu [11]. Developing these two ideas, Domelevo and Omnes in [13] introduced the DDFV schemes for the Laplace equation and established the fundamental duality property between discrete gradient and discrete divergence. Andreianov, Boyer and Hubert extended the DDFV scheme to more general diffusion operators in [5] and proved its convergence. In Section 2, we present a DDFV scheme for the system (5)–(6). Therefore, we introduce the different meshes, the discrete operators and we recall the discrete duality formula. As there is a convection term in (6), we also need to define a discrete convection operator, as in [4] or [10].

In Section 3, we study the stability of the scheme. We prove some a priori estimates on the pressure, the gradient of the pressure, the Darcy velocity (Lemma 3.2) and also a priori estimates on the concentration and the gradient of the concentration (Lemma 3.3). It yields the existence and uniqueness of the approximate solution (Theorem 3.4). Section 4 is devoted to the presentation of some numerical experiments. It shows good results when the permeability

is continuous or has discontinuities supported by the edges of the diamond mesh. However, as it is more natural that the discontinuities of the permeability are supported by the edges of the primal mesh, we introduce a modified DDFV scheme in Section 5. The m-DDFV scheme has been proposed by Hermeline in [26] for 2D linear elliptic problems with discontinuities and extented by Boyer and Hubert in [8] for 2D nonlinear elliptic problems with discontinuities.

Finally, in Section 5.4, we show numerical experiments obtained with the m-DDFV scheme.

2. Presentation of the numerical scheme

2.1. Meshes and notations

In order to define a DDFV scheme, as for instance in [13, 5], we need to introduce three different meshes – the primal mesh, the dual mesh and the diamond mesh – and some associated notations.

The mesh construction starts from the partition $\mathfrak{M}$, the partition of the computational domain Ω, with disjoint open polygonal control volumes $\mathcal{K} \subset \Omega$ such that $\cup\bar{\mathcal{K}} = \bar{\Omega}$. This partition $\mathfrak{M}$ is called the interior primal mesh. We denote by $\partial\mathfrak{M}$ the set of boundary edges, which are considered as degenerate control volumes. Then, the primal mesh is composed of $\mathfrak{M} \cup \partial\mathfrak{M}$, denoted by $\overline{\mathfrak{M}}$. To construct the two others meshes, we need to associate at each primal cell $\mathcal{K} \in \overline{\mathfrak{M}}$, a point $x_\mathcal{K} \in \mathcal{K}$, called the center of the primal cell. Notice that for $\mathcal{K}$ is a degenerate control volume, the point $x_\mathcal{K}$ is necessarily the midpoint of $\mathcal{K}$. This family of centers is denoted by $X = \{x_\mathcal{K}, \mathcal{K} \in \overline{\mathfrak{M}}\}$ and these will determine the two others meshes.

Let X^* denote the set of the vertices of the primal control volumes in $\overline{\mathfrak{M}}$. Distinguishing the interior vertices from the vertices lying on the boundary, we split X^* into $X^* = X^*_{int} \cup X^*_{ext}$. To any point $x_{\mathcal{K}^*} \in X^*_{int}$, we associate the polygon $\mathcal{K}^*$, whose vertices are $\{x_\mathcal{K} \in X / x_{\mathcal{K}^*} \in \bar{\mathcal{K}}, \mathcal{K} \in \mathfrak{M}\}$. The set of these polygons defines the interior dual mesh denoted by $\mathfrak{M}^*$. To any point $x_{\mathcal{K}^*} \in X^*_{ext}$, we then associate the polygon $\mathcal{K}^*$, whose vertices are $\{x_{\mathcal{K}^*}\} \cup \{x_\mathcal{K} \in X / x_{\mathcal{K}^*} \in \bar{\mathcal{K}}, \mathcal{K} \in \overline{\mathfrak{M}}\}$. The set of these polygons is denoted by $\partial\mathfrak{M}^*$ called the boundary dual mesh and the dual mesh is $\mathfrak{M}^* \cup \partial\mathfrak{M}^*$, denoted by $\overline{\mathfrak{M}^*}$.

Assumption: Each primal cell $\mathcal{K} \in \mathfrak{M}$ is star-shaped with respect to $x_\mathcal{K}$ and each dual cell $\mathcal{K}^* \in \overline{\mathfrak{M}^*}$ is star-shaped with respect to $x_{\mathcal{K}^*}$.

To define the last mesh "the diamond mesh", we first introduce the notion of edges. For all neighboring primal cells $\mathcal{K}$ and $\mathcal{L}$, we assume that $\partial\mathcal{K} \cap \partial\mathcal{L}$ is a segment, corresponding to an edge of the mesh $\mathfrak{M}$, denoted by $\sigma = \mathcal{K}|\mathcal{L}$. Let $\mathcal{E}$ be the set of such edges. We similarly define the edges $\mathcal{E}^*$ of the dual mesh $\overline{\mathfrak{M}^*}$: $\sigma^* = \mathcal{K}^*|\mathcal{L}^*$. Remark that if $\mathcal{K}^* \in \partial\mathfrak{M}^*$, then we have $\partial\mathcal{K}^* = \{\sigma^*, \sigma\}$.

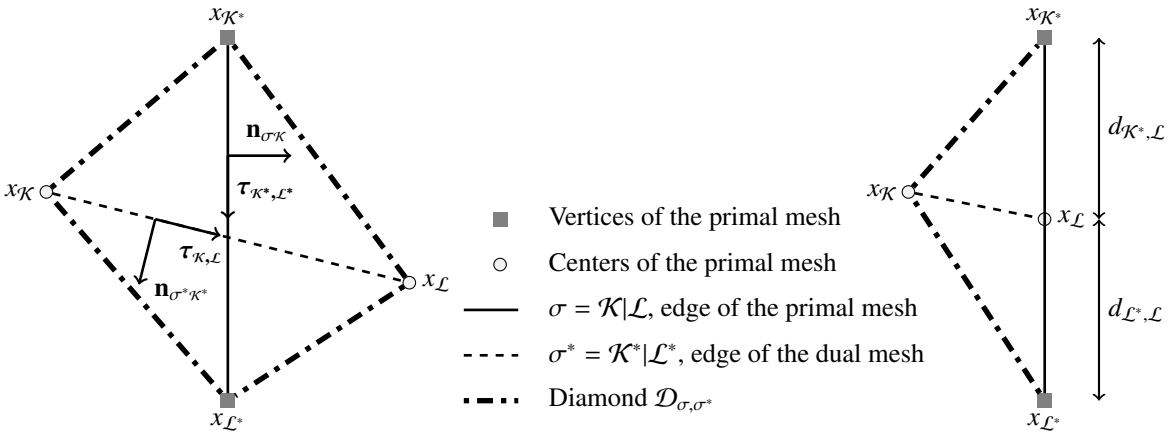

Figure 2.1: Definition of the diamonds $\mathcal{D}_{\sigma,\sigma^*}$

For each couple $(\sigma, \sigma^*) \in \mathcal{E} \times \mathcal{E}^*$ such that $\sigma = \mathcal{K}|\mathcal{L} = (x_{\mathcal{K}^*}, x_{\mathcal{L}^*})$ and $\sigma^* = \mathcal{K}^*|\mathcal{L}^* = (x_\mathcal{K}, x_\mathcal{L})$, we define the quadrilateral diamond cell $\mathcal{D}_{\sigma,\sigma^*}$ whose diagonals are σ and σ^*. If $\sigma \in \mathcal{E} \cap \partial\Omega$, we note that the diamond degenerates

into a triangle. The set of the diamond cells defines the diamond mesh $\mathfrak{D}$. It verifies $\bar{\Omega} = \bigcup_{\mathcal{D}\in\mathfrak{D}} \mathcal{D}$. We have as many diamond cells as primal edges.

Finally, the DDFV mesh is made of the $\mathcal{T} = (\overline{\mathfrak{M}}, \overline{\mathfrak{M}^*})$ and $\mathfrak{D}$. Let us now introduce some notations associated to the meshes $\mathcal{T}$ and $\mathfrak{D}$. For each primal or dual cell V ($V \in \overline{\mathfrak{M}}$ or $V \in \overline{\mathfrak{M}^*}$), we define m_V the measure of V, $\mathcal{E}_V$ the set of the edges of V (it coincides with the edge $\sigma = V$ if $V \in \partial\mathfrak{M}$), $\mathfrak{D}_V$ the set of diamonds $\mathcal{D}_{\sigma,\sigma^*} \in \mathfrak{D}$ such that $\mathrm{m}(\mathcal{D}_{\sigma,\sigma^*} \cap V) > 0$, and d_V the diameter of V.

For a diamond $\mathcal{D}_{\sigma,\sigma^*}$, whose vertices are $(x_\mathcal{K}, x_{\mathcal{K}^*}, x_\mathcal{L}, x_{\mathcal{L}^*})$, we define, as shown on Figure 2.1: $x_\mathcal{D}$ the center of the diamond cell $\mathcal{D}$: $x_\mathcal{D} = \sigma \cap \sigma^*$, m_σ the length of the primal edge σ, m_{σ^*} the length of the dual edge σ^*, $\mathrm{m}_\mathcal{D}$ the measure of $\mathcal{D}$, $d_\mathcal{D}$ its diameter, $\alpha_\mathcal{D}$ the angle between $(x_\mathcal{K}, x_\mathcal{L})$ and $(x_{\mathcal{K}^*}, x_{\mathcal{L}^*})$, $m_{\mathcal{D}_\mathcal{K}}$ the measure of $\mathcal{D} \cap \mathcal{K}$ and $m_{\mathcal{D}_{\mathcal{K}^*}}$ the measure of $\mathcal{D} \cap \mathcal{K}^*$. We will also use two direct basis $(\boldsymbol{\tau}_{\mathcal{K}^*,\mathcal{L}^*}, \mathbf{n}_{\sigma\mathcal{K}})$ and $(\mathbf{n}_{\sigma^*\mathcal{K}^*}, \boldsymbol{\tau}_{\mathcal{K},\mathcal{L}})$, where $\mathbf{n}_{\sigma\mathcal{K}}$ is the unit normal to σ, outward $\mathcal{K}$, $\mathbf{n}_{\sigma^*\mathcal{K}^*}$ is the unit normal to σ^*, outward $\mathcal{K}^*$, $\boldsymbol{\tau}_{\mathcal{K}^*,\mathcal{L}^*}$ is the unit tangent vector to σ, oriented from $\mathcal{K}^*$ to $\mathcal{L}^*$, $\boldsymbol{\tau}_{\mathcal{K},\mathcal{L}}$ is the unit tangent vector to σ^*, oriented from $\mathcal{K}$ to $\mathcal{L}$. For $\sigma = [x_{\mathcal{K}^*}, x_{\mathcal{L}^*}] \in \partial\mathfrak{M}$, we define $d_{\mathcal{K}^*,\mathcal{L}}$ the length of the segment $[x_{\mathcal{K}^*}, x_\mathcal{L}]$and $d_{\mathcal{L}^*,\mathcal{L}}$ the length of the segment $[x_{\mathcal{L}^*}, x_\mathcal{L}]$.

We introduce now the size of the mesh, $\mathrm{size}(\mathcal{T}) = \max_{\mathcal{D}\in\mathfrak{D}} d_\mathcal{D}$. To measure how flat the diamond cells can be, we note $\alpha_\mathcal{T}$ the unique real in $]0, \frac{\pi}{2}]$ such that $\sin(\alpha_\mathcal{T}) := \min_{\mathcal{D}\in\mathfrak{D}}(|\sin(\alpha_\mathcal{D})|)$. We also need some regularity of the mesh, as in [5], which gives the existence of a constant $\zeta > 0$ such that

$$\sum_{\mathcal{D}\in\mathfrak{D}_\mathcal{K}} \mathrm{m}_\sigma m_{\sigma^*} \le \frac{\mathrm{m}_\mathcal{K}}{\zeta}, \forall \mathcal{K} \in \mathfrak{M}, \qquad \text{and} \qquad \sum_{\mathcal{D}\in\mathfrak{D}_{\mathcal{K}^*}} \mathrm{m}_\sigma m_{\sigma^*} \le \frac{\mathrm{m}_{\mathcal{K}^*}}{\zeta}, \forall \mathcal{K}^* \in \overline{\mathfrak{M}^*}. \tag{13}$$

2.2. Discrete operators and duality formula

We define several types of degrees of freedom to represent scalar, vector and **tensor** fields in the discrete setting. We consider :

- $\mathbb{R}^\mathcal{T}$ is a linear space of scalar fields constant on the cells of $\overline{\mathfrak{M}}$ and $\overline{\mathfrak{M}^*}$:

$$\mathbb{R}^\mathcal{T} = \left\{ u_\mathcal{T} = \left((u_\mathcal{K})_{\mathcal{K}\in\overline{\mathfrak{M}}}, (u_{\mathcal{K}^*})_{\mathcal{K}^*\in\overline{\mathfrak{M}^*}} \right), \text{ with } u_\mathcal{K} \in \mathbb{R}, \ \forall \mathcal{K} \in \overline{\mathfrak{M}}, \text{ and } u_{\mathcal{K}^*} \in \mathbb{R}, \ \forall \mathcal{K}^* \in \overline{\mathfrak{M}^*} \right\}.$$

- $\left(\mathbb{R}^2\right)^\mathfrak{D}$ is a linear space of vector fields constant on the cells of $\mathfrak{D}$:

$$\left(\mathbb{R}^2\right)^\mathfrak{D} = \left\{ \boldsymbol{\xi}_\mathfrak{D} = (\boldsymbol{\xi}_\mathcal{D})_{\mathcal{D}\in\mathfrak{D}}, \text{ with } \boldsymbol{\xi}_\mathcal{D} \in \mathbb{R}^2, \ \forall \mathcal{D} \in \mathfrak{D} \right\}.$$

In this section, we recall the definition of two discrete operators. The discrete gradient has been introduced in [12] and further with the discrete divergence in [13]. In order to write a discrete duality property (similar to the Green formula at the discrete level), we also introduce some trace operators and scalar products.

Definition 2.1. *The discrete gradient $\nabla^\mathfrak{D}$ is a mapping from $\mathbb{R}^\mathcal{T}$ to $\left(\mathbb{R}^2\right)^\mathfrak{D}$ defined for all $u_\mathcal{T} \in \mathbb{R}^\mathcal{T}$ by $\nabla^\mathfrak{D} u_\mathcal{T} = \left(\nabla^\mathcal{D} u_\mathcal{T}\right)_{\mathcal{D}\in\mathfrak{D}}$, where for $\mathcal{D} \in \mathfrak{D}$:*

$$\begin{cases} \nabla^\mathcal{D} u_\mathcal{T} \cdot \boldsymbol{\tau}_{\mathcal{K}^*,\mathcal{L}^*} = & \dfrac{u_{\mathcal{L}^*} - u_{\mathcal{K}^*}}{\mathrm{m}_\sigma}, \\ \nabla^\mathcal{D} u_\mathcal{T} \cdot \boldsymbol{\tau}_{\mathcal{K},\mathcal{L}} = & \dfrac{u_\mathcal{L} - u_\mathcal{K}}{m_{\sigma^*}}. \end{cases} \iff \nabla^\mathcal{D} u_\mathcal{T} = \frac{1}{\sin(\alpha_\mathcal{D})} \left(\frac{u_\mathcal{L} - u_\mathcal{K}}{m_{\sigma^*}} \mathbf{n}_{\sigma\mathcal{K}} + \frac{u_{\mathcal{L}^*} - u_{\mathcal{K}^*}}{\mathrm{m}_\sigma} \mathbf{n}_{\sigma^*\mathcal{K}^*} \right)$$

As the measure $\mathrm{m}_\mathcal{D}$ of the diamond $\mathcal{D}$ verifies : $\mathrm{m}_\mathcal{D} = \frac{1}{2} \mathrm{m}_\sigma m_{\sigma^*} \sin(\alpha_\mathcal{D})$, the discrete gradient on $\mathcal{D}$ rewrites:

$$\nabla^\mathcal{D} u_\mathcal{T} = \frac{1}{2\mathrm{m}_\mathcal{D}} \Big[(u_\mathcal{L} - u_\mathcal{K}) \mathrm{m}_\sigma \mathbf{n}_{\sigma\mathcal{K}} + (u_{\mathcal{L}^*} - u_{\mathcal{K}^*}) m_{\sigma^*} \mathbf{n}_{\sigma^*\mathcal{K}^*} \Big].$$

Applying the Green formula to a regular function $\boldsymbol{\xi} : \Omega \to \mathbb{R}^2$, we get:

$$\int_{\mathcal{K}} \mathrm{div}(\boldsymbol{\xi}(x))\mathrm{d}x = \sum_{\sigma\in\partial\mathcal{K}} \int_{\sigma} \boldsymbol{\xi}(s)\cdot\mathbf{n}_{\sigma\mathcal{K}}\mathrm{d}s, \qquad \forall \mathcal{K}\in\mathfrak{M}, \tag{14}$$

and a similar equality when integrating over $\mathcal{K}^* \in \overline{\mathfrak{M}^*}$. Therefore, the discrete divergence $\mathrm{div}^{\mathcal{T}}$ is defined by mimicking (14) at the discrete level.

Definition 2.2. *The discrete divergence operator* $\mathrm{div}^{\mathcal{T}}$ *is a mapping from* $\left(\mathbb{R}^2\right)^{\mathfrak{D}}$ *to* $\mathbb{R}^{\mathcal{T}}$ *defined for all* $\boldsymbol{\xi}_{\mathfrak{D}} \in \left(\mathbb{R}^2\right)^{\mathfrak{D}}$ *by*

$$\mathrm{div}^{\mathcal{T}}\boldsymbol{\xi}_{\mathfrak{D}} = \left(\mathrm{div}^{\mathfrak{M}}\boldsymbol{\xi}_{\mathfrak{D}}, \mathrm{div}^{\partial\mathfrak{M}}\boldsymbol{\xi}_{\mathfrak{D}}, \mathrm{div}^{\mathfrak{M}^*}\boldsymbol{\xi}_{\mathfrak{D}}, \mathrm{div}^{\partial\mathfrak{M}^*}\boldsymbol{\xi}_{\mathfrak{D}}\right),$$

with $\mathrm{div}^{\mathfrak{M}}\boldsymbol{\xi}_{\mathfrak{D}} = (\mathrm{div}_{\mathcal{K}}\boldsymbol{\xi}_{\mathfrak{D}})_{\mathcal{K}\in\mathfrak{M}}$, $\mathrm{div}^{\partial\mathfrak{M}}\boldsymbol{\xi}_{\mathfrak{D}} = 0$, $\mathrm{div}^{\mathfrak{M}^*}\boldsymbol{\xi}_{\mathfrak{D}} = (\mathrm{div}_{\mathcal{K}^*}\boldsymbol{\xi}_{\mathfrak{D}})_{\mathcal{K}^*\in\mathfrak{M}^*}$ *and* $\mathrm{div}^{\partial\mathfrak{M}^*}\boldsymbol{\xi}_{\mathfrak{D}} = (\mathrm{div}_{\mathcal{K}^*}\boldsymbol{\xi}_{\mathfrak{D}})_{\mathcal{K}^*\in\partial\mathfrak{M}^*}$ *such that:*

$$\begin{aligned}
\forall\, \mathcal{K}\in\mathfrak{M}, \qquad \mathrm{div}_{\mathcal{K}}\boldsymbol{\xi}_{\mathfrak{D}} &= \frac{1}{\mathrm{m}_{\mathcal{K}}} \sum_{\substack{\mathcal{D}\in\mathfrak{D}_{\mathcal{K}}\\ \mathcal{D}=\mathcal{D}_{\sigma,\sigma^*}}} \mathrm{m}_{\sigma}\,\boldsymbol{\xi}_{\mathcal{D}}\cdot\mathbf{n}_{\sigma\mathcal{K}},\\
\forall\, \mathcal{K}^*\in\mathfrak{M}^*, \qquad \mathrm{div}_{\mathcal{K}^*}\boldsymbol{\xi}_{\mathfrak{D}} &= \frac{1}{\mathrm{m}_{\mathcal{K}^*}} \sum_{\substack{\mathcal{D}\in\mathfrak{D}_{\mathcal{K}^*}\\ \mathcal{D}=\mathcal{D}_{\sigma,\sigma^*}}} m_{\sigma^*}\,\boldsymbol{\xi}_{\mathcal{D}}\cdot\mathbf{n}_{\sigma^*\mathcal{K}^*},\\
\forall\, \mathcal{K}^*\in\partial\mathfrak{M}^*, \quad \mathrm{div}_{\mathcal{K}^*}\boldsymbol{\xi}_{\mathfrak{D}} &= \frac{1}{\mathrm{m}_{\mathcal{K}^*}} \left(\sum_{\substack{\mathcal{D}\in\mathfrak{D}_{\mathcal{K}^*}\\ \mathcal{D}=\mathcal{D}_{\sigma,\sigma^*}}} m_{\sigma^*}\,\boldsymbol{\xi}_{\mathcal{D}}\cdot\mathbf{n}_{\sigma^*\mathcal{K}^*} + \sum_{\substack{\mathcal{D}\in\mathfrak{D}_{\mathcal{K}^*}\cap\mathfrak{D}_{ext}\\ \mathcal{D}=\mathcal{D}_{\sigma,\sigma^*}}} d_{\mathcal{K}^*,\mathcal{L}}\,\boldsymbol{\xi}_{\mathcal{D}}\cdot\mathbf{n}_{\sigma\mathcal{K}} \right).
\end{aligned}$$

Let us now introduce two trace operators, defined respectively on $\mathbb{R}^{\mathcal{T}}$ and $\left(\mathbb{R}^2\right)^{\mathfrak{D}}$. The first one is $\gamma^{\mathcal{T}} : u_{\mathcal{T}} \in \mathbb{R}^{\mathcal{T}} \mapsto \gamma^{\mathcal{T}}(u_{\mathcal{T}}) = \left(\gamma_{\sigma}(u_{\mathcal{T}})\right)_{\sigma\in\partial\mathfrak{M}} \in \mathbb{R}^{\partial\mathfrak{M}}$, defined by :

$$\gamma_{\sigma}(u_{\mathcal{T}}) = \frac{d_{\mathcal{K}^*,\mathcal{L}}(u_{\mathcal{K}^*}+u_{\mathcal{L}}) + d_{\mathcal{L}^*,\mathcal{L}}(u_{\mathcal{L}^*}+u_{\mathcal{L}})}{2\mathrm{m}_{\sigma}}, \qquad \forall\, \sigma = [x_{\mathcal{K}^*}, x_{\mathcal{L}^*}] \in \partial\mathfrak{M}. \tag{15}$$

The second one is $\gamma^{\mathfrak{D}} : \boldsymbol{\varphi}^{\mathfrak{D}} \in (\mathbb{R}^2)^{\mathfrak{D}} \mapsto (\boldsymbol{\varphi}_{\mathcal{D}})_{\mathcal{D}\in\mathfrak{D}_{ext}} \in (\mathbb{R}^2)^{\mathfrak{D}_{ext}}$.

In order to show the duality property between the discrete gradient and the discrete divergence, we define the scalar products $[\![\cdot,\cdot]\!]_{\mathcal{T}}$ on $\mathbb{R}^{\mathcal{T}}$ and $(\cdot,\cdot)_{\mathfrak{D}}$ on $\left(\mathbb{R}^2\right)^{\mathfrak{D}}$ by

$$\begin{aligned}
[\![v_{\mathcal{T}}, u_{\mathcal{T}}]\!]_{\mathcal{T}} &= \frac{1}{2}\left(\sum_{\mathcal{K}\in\mathfrak{M}} \mathrm{m}_{\mathcal{K}} u_{\mathcal{K}} v_{\mathcal{K}} + \sum_{\mathcal{K}^*\in\overline{\mathfrak{M}^*}} \mathrm{m}_{\mathcal{K}^*} u_{\mathcal{K}^*} v_{\mathcal{K}^*} \right), \quad \forall u_{\mathcal{T}}, v_{\mathcal{T}} \in \mathbb{R}^{\mathcal{T}},\\
(\boldsymbol{\xi}_{\mathfrak{D}}, \boldsymbol{\varphi}_{\mathfrak{D}})_{\mathfrak{D}} &= \sum_{\mathcal{D}\in\mathfrak{D}} \mathrm{m}_{\mathcal{D}}\,\boldsymbol{\xi}_{\mathcal{D}}\cdot\boldsymbol{\varphi}_{\mathcal{D}}, \quad \forall \boldsymbol{\xi}_{\mathfrak{D}}, \boldsymbol{\varphi}_{\mathfrak{D}} \in \left(\mathbb{R}^2\right)^{\mathfrak{D}}.
\end{aligned}$$

The corresponding norms are denoted by $\|\cdot\|_{2,\mathcal{T}}$ and $\|\cdot\|_{2,\mathfrak{D}}$. More generally, we set:

$$\begin{aligned}
\|u_{\mathcal{T}}\|_{p,\mathcal{T}} &= \left(\frac{1}{2}\sum_{\mathcal{K}\in\mathfrak{M}} \mathrm{m}_{\mathcal{K}} |u_{\mathcal{K}}|^p + \frac{1}{2}\sum_{\mathcal{K}^*\in\overline{\mathfrak{M}^*}} \mathrm{m}_{\mathcal{K}^*} |u_{\mathcal{K}^*}|^p \right)^{1/p}, \quad \forall u_{\mathcal{T}} \in \mathbb{R}^{\mathcal{T}},\ \forall 1 \le p < +\infty\\
\|u_{\mathcal{T}}\|_{\infty,\mathcal{T}} &= \max\left(\max_{\mathcal{K}\in\overline{\mathfrak{M}}} |u_{\mathcal{K}}|, \max_{\mathcal{K}^*\in\overline{\mathfrak{M}^*}} |u_{\mathcal{K}^*}| \right), \quad \forall u_{\mathcal{T}} \in \mathbb{R}^{\mathcal{T}},\\
\left\|\boldsymbol{\xi}_{\mathfrak{D}}\right\|_{p,\mathfrak{D}} &= \left(\sum_{\mathcal{D}\in\mathfrak{D}} \mathrm{m}_{\mathcal{D}} |\boldsymbol{\xi}_{\mathcal{D}}|^p \right)^{1/p}, \quad \forall \boldsymbol{\xi}_{\mathfrak{D}} \in \left(\mathbb{R}^2\right)^{\mathfrak{D}},\ \forall 1 \le p < +\infty\\
\left\|\boldsymbol{\xi}_{\mathfrak{D}}\right\|_{\infty,\mathfrak{D}} &= \max_{\mathcal{D}\in\mathfrak{D}} \left|\boldsymbol{\xi}_{\mathcal{D}}\right|, \quad \forall \boldsymbol{\xi}_{\mathfrak{D}} \in \left(\mathbb{R}^2\right)^{\mathfrak{D}}.
\end{aligned} \tag{16}$$

We also define $\langle \cdot, \cdot \rangle_{\partial\Omega}$ on $\mathbb{R}^{\mathfrak{D}_{ext}} \times \mathbb{R}^{\partial\mathfrak{M}}$ by

$$\langle \phi_{\mathfrak{D}}, v_{\partial\mathfrak{M}} \rangle_{\partial\Omega} = \sum_{\mathcal{D}_{\sigma,\sigma^*} \in \mathfrak{D}_{ext}} \mathrm{m}_\sigma \phi_{\mathcal{D}} v_\sigma, \quad \forall\, \phi_{\mathfrak{D}} \in \mathbb{R}^{\mathfrak{D}_{ext}}, \forall v_{\partial\mathfrak{M}} = (v_\sigma)_{\sigma \in \partial\mathfrak{M}} \in \mathbb{R}^{\partial\mathfrak{M}}.$$

The basis of the Discrete Duality Finite Volume methods lies on the discrete duality formula recalled in Theorem 2.3 and proved for instance in [13].

Theorem 2.3. *For all* $(\boldsymbol{\xi}_{\mathfrak{D}}, v_{\mathcal{T}}) \in \left(\mathbb{R}^2\right)^{\mathfrak{D}} \times \mathbb{R}^{\mathcal{T}}$*, we have*

$$[\![\mathrm{div}^{\mathcal{T}} \boldsymbol{\xi}_{\mathfrak{D}}, v_{\mathcal{T}}]\!]_{\mathcal{T}} = -(\boldsymbol{\xi}_{\mathfrak{D}}, \nabla^{\mathfrak{D}} v_{\mathcal{T}})_{\mathfrak{D}} + \langle \gamma^{\mathfrak{D}}(\boldsymbol{\xi}_{\mathfrak{D}}) \cdot \mathbf{n}, \gamma^{\mathcal{T}}(v_{\mathcal{T}}) \rangle_{\partial\Omega},$$

where $\mathbf{n}$ *is the exterior unit normal to* Ω*.*

2.3. A discrete convection operator

In order to treat the convection terms in the concentration equation, we define a discrete convection operator. This operator is similar to the one introduced in [4] but is written here for an upwinding of the convection terms.

Definition 2.4. *The discrete convection operator* $\mathrm{divc}^{\mathcal{T}}$ *is a mapping from* $\left(\mathbb{R}^2\right)^{\mathfrak{D}} \times \mathbb{R}^{\mathcal{T}}$ *to* $\mathbb{R}^{\mathcal{T}}$ *defined for all* $\boldsymbol{\xi}_{\mathfrak{D}} \in \left(\mathbb{R}^2\right)^{\mathfrak{D}}$ *and* $v_{\mathcal{T}} \in \mathbb{R}^{\mathcal{T}}$ *by*

$$\mathrm{divc}^{\mathcal{T}}(\boldsymbol{\xi}_{\mathfrak{D}}, v_{\mathcal{T}}) = \left(\mathrm{divc}^{\mathfrak{M}}(\boldsymbol{\xi}_{\mathfrak{D}}, v_{\mathcal{T}}), \mathrm{divc}^{\partial\mathfrak{M}}(\boldsymbol{\xi}_{\mathfrak{D}}, v_{\mathcal{T}}), \mathrm{divc}^{\mathfrak{M}^*}(\boldsymbol{\xi}_{\mathfrak{D}}, v_{\mathcal{T}}), \mathrm{divc}^{\partial\mathfrak{M}^*}(\boldsymbol{\xi}_{\mathfrak{D}}, v_{\mathcal{T}})\right),$$

with $\mathrm{divc}^{\mathfrak{M}}(\boldsymbol{\xi}_{\mathfrak{D}}, v_{\mathcal{T}}) = (\mathrm{divc}_{\mathcal{K}}(\boldsymbol{\xi}_{\mathfrak{D}}, v_{\mathcal{T}}))_{\mathcal{K} \in \mathfrak{M}}$*,* $\mathrm{divc}^{\partial\mathfrak{M}}(\boldsymbol{\xi}_{\mathfrak{D}}, v_{\mathcal{T}}) = 0$*,* $\mathrm{divc}^{\mathfrak{M}^*}(\boldsymbol{\xi}_{\mathfrak{D}}, v_{\mathcal{T}}) = (\mathrm{divc}_{\mathcal{K}^*}(\boldsymbol{\xi}_{\mathfrak{D}}, v_{\mathcal{T}}))_{\mathcal{K}^* \in \mathfrak{M}^*}$ *and* $\mathrm{divc}^{\partial\mathfrak{M}^*}(\boldsymbol{\xi}_{\mathfrak{D}}, v_{\mathcal{T}}) = (\mathrm{divc}_{\mathcal{K}^*}(\boldsymbol{\xi}_{\mathfrak{D}}, v_{\mathcal{T}}))_{\mathcal{K}^* \in \partial\mathfrak{M}^*}$ *such that:*

$$\forall \mathcal{K} \in \mathfrak{M}, \quad \mathrm{divc}_{\mathcal{K}}(\boldsymbol{\xi}_{\mathfrak{D}}, v_{\mathcal{T}}) = \frac{1}{\mathrm{m}_{\mathcal{K}}} \sum_{\mathcal{D}_{\sigma,\sigma^*} \in \mathfrak{D}_{\mathcal{K}}} \mathrm{m}_\sigma \left((\boldsymbol{\xi}_{\mathcal{D}} \cdot \mathbf{n}_{\sigma\mathcal{K}})^+ v_{\mathcal{K}} - (\boldsymbol{\xi}_{\mathcal{D}} \cdot \mathbf{n}_{\sigma\mathcal{K}})^- v_{\mathcal{L}} \right),$$

$$\forall \mathcal{K}^* \in \mathfrak{M}^*, \quad \mathrm{divc}_{\mathcal{K}^*}(\boldsymbol{\xi}_{\mathfrak{D}}, v_{\mathcal{T}}) = \frac{1}{\mathrm{m}_{\mathcal{K}^*}} \sum_{\mathcal{D}_{\sigma,\sigma^*} \in \mathfrak{D}_{\mathcal{K}^*}} m_{\sigma^*} \left((\boldsymbol{\xi}_{\mathcal{D}} \cdot \mathbf{n}_{\sigma^*\mathcal{K}^*})^+ v_{\mathcal{K}^*} - (\boldsymbol{\xi}_{\mathcal{D}} \cdot \mathbf{n}_{\sigma^*\mathcal{K}^*})^- v_{\mathcal{L}^*} \right),$$

$$\forall \mathcal{K}^* \in \partial\mathfrak{M}^*, \quad \mathrm{divc}_{\mathcal{K}^*}(\boldsymbol{\xi}_{\mathfrak{D}}, v_{\mathcal{T}}) = \frac{1}{\mathrm{m}_{\mathcal{K}^*}} \left(\sum_{\substack{\mathcal{D} \in \mathfrak{D}_{\mathcal{K}^*} \\ \mathcal{D} = \mathcal{D}_{\sigma,\sigma^*}}} m_{\sigma^*} \left((\boldsymbol{\xi}_{\mathcal{D}} \cdot \mathbf{n}_{\sigma^*\mathcal{K}^*})^+ v_{\mathcal{K}^*} - (\boldsymbol{\xi}_{\mathcal{D}} \cdot \mathbf{n}_{\sigma^*\mathcal{K}^*})^- v_{\mathcal{L}^*} \right) \right.$$
$$\left. + \sum_{\substack{\mathcal{D} \in \mathfrak{D}_{\mathcal{K}^*} \cap \mathfrak{D}_{ext} \\ \mathcal{D} = \mathcal{D}_{\sigma,\sigma^*}}} d_{\mathcal{K}^*,\mathcal{L}} \left((\boldsymbol{\xi}_{\mathcal{D}} \cdot \mathbf{n}_{\sigma\mathcal{K}})^+ v_{\mathcal{K}} - (\boldsymbol{\xi}_{\mathcal{D}} \cdot \mathbf{n}_{\sigma\mathcal{K}})^- v_{\mathcal{L}} \right) \right),$$

where $x^+ = \max(x, 0)$ *and* $x^- = -\min(x, 0)$ *for all* $x \in \mathbb{R}$*.*

This discrete convection operator satisfies the discrete property stated in Lemma 2.5.

Lemma 2.5. *For all* $u_{\mathcal{T}} \in \mathbb{R}^{\mathcal{T}}$ *and* $\mathbf{b}_{\mathfrak{D}} \in \left(\mathbb{R}^2\right)^{\mathfrak{D}}$ *verifying* $\mathbf{b}_{\mathcal{D}} \cdot \mathbf{n} = 0$ *for all* $\mathcal{D} \in \mathfrak{D}_{ext}$*, we have:*

$$[\![\mathrm{divc}^{\mathcal{T}}(\mathbf{b}_{\mathfrak{D}}, u_{\mathcal{T}}), u_{\mathcal{T}}]\!]_{\mathcal{T}} \geq \frac{1}{2} [\![\mathrm{div}^{\mathcal{T}}(\mathbf{b}_{\mathfrak{D}}), (u_{\mathcal{T}})^2]\!]_{\mathcal{T}}.$$

Proof. Due to the definition of the scalar product $[\![\cdot, \cdot]\!]_{\mathcal{T}}$, the quantity $[\![\mathrm{divc}^{\mathcal{T}}(\mathbf{b}_{\mathfrak{D}}, u_{\mathcal{T}}), u_{\mathcal{T}}]\!]_{\mathcal{T}}$ is the sum of a primal term T_p and a dual term T_d. We first consider the primal term:

$$\begin{aligned} T_p = & \frac{1}{2} \sum_{\mathcal{K} \in \mathfrak{M}} \mathrm{m}_{\mathcal{K}} \mathrm{divc}_{\mathcal{K}}(\mathbf{b}_{\mathfrak{D}}, u_{\mathcal{T}}) u_{\mathcal{K}}, \\ = & \frac{1}{2} \sum_{\mathcal{K} \in \mathfrak{M}} \sum_{\mathcal{D}_{\sigma,\sigma^*} \in \mathfrak{D}_{\mathcal{K}}} \mathrm{m}_\sigma \left((\mathbf{b}_{\mathcal{D}} \cdot \mathbf{n}_{\sigma\mathcal{K}})^+ u_{\mathcal{K}} - (\mathbf{b}_{\mathcal{D}} \cdot \mathbf{n}_{\sigma\mathcal{K}})^- u_{\mathcal{L}} \right) u_{\mathcal{K}} \end{aligned}$$

Rewriting T_p as a sum on all the primal edges of the mesh and using the relations $|x| = x^+ + x^-$, $x = x^+ - x^-$ and $(a-b)a = \frac{1}{2}((a-b)^2 + a^2 - b^2)$, we get:

$$\begin{aligned} T_p = & \frac{1}{2} \sum_{\mathcal{D}_{\sigma,\sigma^*} \in \mathfrak{D}} \mathrm{m}_\sigma \left((\mathbf{b}_\mathcal{D} \cdot \mathbf{n}_{\sigma\mathcal{K}})^+ u_\mathcal{K} - (\mathbf{b}_\mathcal{D} \cdot \mathbf{n}_{\sigma\mathcal{K}})^- u_\mathcal{L} \right) (u_\mathcal{K} - u_\mathcal{L}) \\ = & \frac{1}{2} \sum_{\mathcal{D}_{\sigma,\sigma^*} \in \mathfrak{D}} \mathrm{m}_\sigma \left(|\mathbf{b}_\mathcal{D} \cdot \mathbf{n}_{\sigma\mathcal{K}}| u_\mathcal{K} (u_\mathcal{K} - u_\mathcal{L}) - (\mathbf{b}_\mathcal{D} \cdot \mathbf{n}_{\sigma\mathcal{K}})^- (u_\mathcal{K}^2 - u_\mathcal{L}^2) \right) \\ = & \frac{1}{4} \left(\sum_{\mathcal{D}_{\sigma,\sigma^*} \in \mathfrak{D}} \mathrm{m}_\sigma |\mathbf{b}_\mathcal{D} \cdot \mathbf{n}_{\sigma\mathcal{K}}| (u_\mathcal{K} - u_\mathcal{L})^2 + \sum_{\mathcal{D}_{\sigma,\sigma^*} \in \mathfrak{D}} \mathrm{m}_\sigma \mathbf{b}_\mathcal{D} \cdot \mathbf{n}_{\sigma\mathcal{K}} (u_\mathcal{K}^2 - u_\mathcal{L}^2) \right) \end{aligned}$$

The first term in the sum is clearly nonnegative and the second term can be rewritten thanks to a discrete integration by parts leading to

$$T_p \geq \frac{1}{4} \sum_{\mathcal{K} \in \mathfrak{M}} \mathrm{m}_\mathcal{K} u_\mathcal{K}^2 \mathrm{div}_\mathcal{K}(\mathbf{b}_\mathfrak{D}). \tag{17}$$

For the dual term, we have:

$$\begin{aligned} T_d = & \frac{1}{2} \sum_{\mathcal{K}^* \in \overline{\mathfrak{M}^*}} \mathrm{m}_{\mathcal{K}^*} \mathrm{divc}_{\mathcal{K}^*}(\mathbf{b}_\mathfrak{D}, u_\mathcal{T}) u_{\mathcal{K}^*} \\ = & \frac{1}{2} \sum_{\mathcal{K}^* \in \overline{\mathfrak{M}^*}} \sum_{\mathcal{D}_{\sigma,\sigma^*} \in \mathfrak{D}_{\mathcal{K}^*}} m_{\sigma^*} \left((\mathbf{b}_\mathcal{D} \cdot \mathbf{n}_{\sigma^*\mathcal{K}^*})^+ u_{\mathcal{K}^*} - (\mathbf{b}_\mathcal{D} \cdot \mathbf{n}_{\sigma^*\mathcal{K}^*})^- u_{\mathcal{L}^*} \right) u_{\mathcal{K}^*} \end{aligned}$$

because the boundary terms vanish due to the hypothesis $\mathbf{b}_\mathcal{D} \cdot \mathbf{n} = 0$ for all $\mathcal{D} \in \mathfrak{D}_{ext}$. Then, T_d can be rewritten as a sum on the dual edges and following the same computations as for T_p, we get

$$T_d \geq \frac{1}{4} \sum_{\mathcal{K}^* \in \overline{\mathfrak{M}^*}} \mathrm{m}_{\mathcal{K}^*} u_{\mathcal{K}^*}^2 \mathrm{div}_{\mathcal{K}^*}(\mathbf{b}_\mathfrak{D}). \tag{18}$$

Thanks to (17), (18) and the equality

$$\frac{1}{4} \sum_{\mathcal{K} \in \mathfrak{M}} \mathrm{m}_\mathcal{K} u_\mathcal{K}^2 \mathrm{div}_\mathcal{K}(\mathbf{b}_\mathfrak{D}) + \frac{1}{4} \sum_{\mathcal{K}^* \in \overline{\mathfrak{M}^*}} \mathrm{m}_{\mathcal{K}^*} u_{\mathcal{K}^*}^2 \mathrm{div}_{\mathcal{K}^*}(\mathbf{b}_\mathfrak{D}) = \frac{1}{2} [\![\mathrm{div}^\mathcal{T}(\mathbf{b}_\mathfrak{D}), (u_\mathcal{T})^2]\!]_\mathcal{T},$$

the proof is ended.

□

2.4. The numerical scheme

Let $(\mathcal{T}, \mathfrak{D})$ be a DDFV mesh of Ω (as presented in Section 2.1) and $\delta t > 0$ be a time step. In order to compute a numerical approximation to (5)–(6) on $]0, T[\times \Omega$, we set $N_T = T/\delta t$ (we always choose time steps such that N_T is an integer) and we define $t_n = n\delta t$ for $n \in \{0, \dots, N_T\}$.

First, we discretize all the data of the problem. Therefore, we introduce $\mathbb{P}_\mathcal{K}$ (respectively $\mathbb{P}_{\mathcal{K}^*}$) the L^2 projection over an interior primal cell (respectively a dual cell). We then define $c_\mathcal{T}^0 = \left((\mathbb{P}_\mathcal{K} c_0)_{\mathcal{K} \in \mathfrak{M}}, 0, (\mathbb{P}_{\mathcal{K}^*} c_0)_{\mathcal{K}^* \in \overline{\mathfrak{M}^*}} \right) \in \mathbb{R}^\mathcal{T}$ and $\Phi_\mathcal{T} = \left((\mathbb{P}_\mathcal{K} \Phi)_{\mathcal{K} \in \mathfrak{M}}, 0, (\mathbb{P}_{\mathcal{K}^*} \Phi)_{\mathcal{K}^* \in \overline{\mathfrak{M}^*}} \right) \in \mathbb{R}^\mathcal{T}$. In a similar way, for all $n \geq 1$, we define $(q_\mathcal{T}^{+,n}, q_\mathcal{T}^{-,n}, \hat{c}_\mathcal{T}^n) \in (\mathbb{R}^\mathcal{T})^3$ by taking the mean values of q^+, q^- and $\hat{c}$ on the primal and dual cells crossed with the time interval (t_{n-1}, t_n):

$$\begin{aligned} q_\mathcal{T}^{+,n} &= \frac{1}{\delta t} \int_{t_{n-1}}^{t_n} \left((\mathbb{P}_\mathcal{K} q^+(.,t))_{\mathcal{K} \in \mathfrak{M}}, 0, (\mathbb{P}_{\mathcal{K}^*} q^+(.,t))_{\mathcal{K}^* \in \overline{\mathfrak{M}^*}} \right) dt \\ q_\mathcal{T}^{-,n} &= \frac{1}{\delta t} \int_{t_{n-1}}^{t_n} \left((\mathbb{P}_\mathcal{K} q^-(.,t))_{\mathcal{K} \in \mathfrak{M}}, 0, (\mathbb{P}_{\mathcal{K}^*} q^-(.,t))_{\mathcal{K}^* \in \overline{\mathfrak{M}^*}} \right) dt \\ \hat{c}_\mathcal{T}^n &= \frac{1}{\delta t} \int_{t_{n-1}}^{t_n} \left((\mathbb{P}_\mathcal{K} \hat{c}(.,t))_{\mathcal{K} \in \mathfrak{M}}, 0, (\mathbb{P}_{\mathcal{K}^*} \hat{c}(.,t))_{\mathcal{K}^* \in \overline{\mathfrak{M}^*}} \right) dt. \end{aligned}$$

At each time step n, the numerical solution will be given by $(p_{\mathcal{T}}^n, \mathbf{U}_{\mathfrak{D}}^n, c_{\mathcal{T}}^n) \in \mathbb{R}^{\mathcal{T}} \times \left(\mathbb{R}^2\right)^{\mathfrak{D}} \times \mathbb{R}^{\mathcal{T}}$ and the computation of the pressure is decoupled from the computation of the concentration. From the approximate concentration given on primal and dual cells $c_{\mathcal{T}}^{n-1}$, we reconstruct some approximate values on each diamond cell

$$c_{\mathcal{D}}^{n-1} = \frac{m_{\mathcal{D}_{\mathcal{K}}}}{2\mathrm{m}_{\mathcal{D}}} c_{\mathcal{K}}^{n-1} + \frac{m_{\mathcal{D}_{\mathcal{K}^*}}}{2\mathrm{m}_{\mathcal{D}}} c_{\mathcal{K}^*}^{n-1} + \frac{m_{\mathcal{D}_{\mathcal{L}}}}{2\mathrm{m}_{\mathcal{D}}} c_{\mathcal{L}}^{n-1} + \frac{m_{\mathcal{D}_{\mathcal{L}^*}}}{2\mathrm{m}_{\mathcal{D}}} c_{\mathcal{L}^*}^{n-1}.$$

We introduce the new vector $c_{\mathfrak{D}}^{n-1} = (c_{\mathcal{D}}^{n-1})_{\mathcal{D}\in\mathfrak{D}}$, the approximate tensors

$$\mathbb{A}_{\mathcal{D}}(s) = \frac{1}{\mathrm{m}_{\mathcal{D}}} \int_{\mathcal{D}} \mathbb{A}(x,s)dx \ \forall s \in \mathbb{R}, \quad \mathbb{D}_{\mathcal{D}}(\mathbf{W}) = \frac{1}{\mathrm{m}_{\mathcal{D}}} \int_{\mathcal{D}} \mathbb{D}(x,\mathbf{W})dx, \ \forall \mathbf{W} \in \mathbb{R}^2,$$

and $\mathbb{A}_{\mathfrak{D}}(c_{\mathfrak{D}}^{n-1}) = \left(\mathbb{A}_{\mathcal{D}}(c_{\mathcal{D}}^{n-1})\right)_{\mathcal{D}\in\mathfrak{D}}$ and $\mathbb{D}_{\mathfrak{D}}\left(\mathbf{U}_{\mathfrak{D}}^n\right) = \left(\mathbb{D}_{\mathcal{D}}(\mathbf{U}_{\mathcal{D}}^n)\right)_{\mathcal{D}\in\mathfrak{D}}$.

Then, the scheme for (5) writes $\forall 1 \le n \le N_T$

$$\mathrm{div}^{\mathcal{T}}\left(\mathbf{U}_{\mathfrak{D}}^n\right) = q_{\mathcal{T}}^{+,n} - q_{\mathcal{T}}^{-,n}, \tag{19}$$

$$\mathbf{U}_{\mathfrak{D}}^n = -\mathbb{A}_{\mathfrak{D}}(c_{\mathfrak{D}}^{n-1})\nabla^{\mathfrak{D}} p_{\mathcal{T}}^n, \tag{20}$$

$$\mathbf{U}_{\mathcal{D}}^n \cdot \mathbf{n} = 0, \quad \forall \mathcal{D} \in \mathfrak{D}_{ext}, \tag{21}$$

$$\sum_{\mathcal{K}\in\mathfrak{M}} \mathrm{m}_{\mathcal{K}} p_{\mathcal{K}}^n = \sum_{\mathcal{K}^*\in\overline{\mathfrak{M}^*}} \mathrm{m}_{\mathcal{K}^*} p_{\mathcal{K}^*}^n = 0, \tag{22}$$

and the scheme for (6) writes $\forall 1 \le n \le N_T$

$$\Phi_{\mathcal{T}} \frac{c_{\mathcal{T}}^n - c_{\mathcal{T}}^{n-1}}{\delta t} - \mathrm{div}^{\mathcal{T}}\left(\mathbb{D}_{\mathfrak{D}}\left(\mathbf{U}_{\mathfrak{D}}^n\right)\nabla^{\mathfrak{D}} c_{\mathcal{T}}^n\right) + \mathrm{divc}^{\mathcal{T}}\left(\mathbf{U}_{\mathfrak{D}}^n, c_{\mathcal{T}}^n\right) + q_{\mathcal{T}}^{-,n} c_{\mathcal{T}}^n = q_{\mathcal{T}}^{+,n} \hat{c}_{\mathcal{T}}^n, \tag{23}$$

$$\mathbb{D}_{\mathcal{D}}\left(\mathbf{U}_{\mathcal{D}}^n\right)\nabla^{\mathcal{D}} c_{\mathcal{T}}^n \cdot \mathbf{n} = 0, \forall \mathcal{D} \in \mathfrak{D}_{ext}. \tag{24}$$

The scheme (19)–(24) comes down to a resolution of two linear systems: starting from $c_{\mathcal{T}}^{n-1}$, $(p_{\mathcal{T}}^n, \mathbf{U}_{\mathfrak{D}}^n)$ is obtained by solving the linear system (19)–(22) and then $c_{\mathcal{T}}^n$ is computed by solving the linear system (23)-(24). The inversibility of these linear systems, and then existence and uniqueness of a solution to the linear scheme, will be proved in Section 3.2.

3. A priori estimates and existence and uniqueness result

3.1. A priori estimates

In this Section, we prove *a priori* estimates satisfied by the solution to the scheme (19)–(24). Therefore, we need a discrete Poincaré inequality. This inequality is recalled in Theorem 3.1. We refer to [28] or [7] for its proof.

Theorem 3.1 (Poincaré inequality)**.** *Let Ω be an open bounded polygonal domain of $\mathbb{R}^2$ and $\mathcal{T}$ a DDFV mesh of Ω. There exists $C > 0$ depending only on Ω and on ζ, such that $\forall\ u_{\mathcal{T}} \in \mathbb{R}^{\mathcal{T}}$ with $\sum_{\mathcal{K}\in\mathfrak{M}} \mathrm{m}_{\mathcal{K}} u_{\mathcal{K}} = \sum_{\mathcal{K}^*\in\overline{\mathfrak{M}^*}} \mathrm{m}_{\mathcal{K}^*} u_{\mathcal{K}^*} = 0$, we have*

$$\|u_{\mathcal{T}}\|_{2,\mathcal{T}} \le \frac{C}{\sin(\alpha_{\mathcal{T}})} \|\nabla^{\mathfrak{D}} u_{\mathcal{T}}\|_{2,\mathfrak{D}}.$$

We first establish *a priori estimates* on the pressure, the gradient of the pressure and the Darcy's velocity at the discrete level.

Lemma 3.2. *Let Ω be a convex polygonal domain of $\mathbb{R}^2$ and $\mathcal{T}$ a DDFV mesh of this domain. Assume* (7)–(12) *hold and that the scheme* (19)–(24) *has a solution $(p_{\mathcal{T}}^n, \mathbf{U}_{\mathfrak{D}}^n, c_{\mathcal{T}}^n)_{1\le n\le N_T}$. Then, there exists $C > 0$ depending only on Ω, ζ, $\sin(\alpha_{\mathcal{T}})$, α_A and Λ_A, such that we have for all $n \in [1, \dots, N_T]$:*

$$\left\|p_{\mathcal{T}}^n\right\|_{2,\mathcal{T}} + \left\|\nabla^{\mathfrak{D}} p_{\mathcal{T}}^n\right\|_{2,\mathfrak{D}} + \left\|\mathbf{U}_{\mathfrak{D}}^n\right\|_{2,\mathfrak{D}} \le C\|q^+ - q^-\|_{L^\infty(0,T;L^2(\Omega))}. \tag{25}$$

Proof. We multiply the scheme (19) by $p^n_{\mathcal{T}}$. Thanks to the Neumann boundary condition (21), the discrete duality formula (Theorem 2.3) yields:

$$\left[\!\left[q^{+,n}_{\mathcal{T}} - q^{-,n}_{\mathcal{T}}, p^n_{\mathcal{T}}\right]\!\right]_{\mathcal{T}} = \quad \left[\!\left[\mathrm{div}^{\mathcal{T}}\left(\mathbf{U}^n_{\mathfrak{D}}\right), p^n_{\mathcal{T}}\right]\!\right]_{\mathcal{T}} = -\left(\mathbf{U}^n_{\mathfrak{D}}, \nabla^{\mathfrak{D}} p^n_{\mathcal{T}}\right)_{\mathfrak{D}}.$$

Then, using (20), hypothesis (8) and Cauchy-Schwarz inequality, we have

$$\alpha_A \left\|\nabla^{\mathfrak{D}} p^n_{\mathcal{T}}\right\|^2_{2,\mathfrak{D}} \leq \left[\!\left[q^{+,n}_{\mathcal{T}} - q^{-,n}_{\mathcal{T}}, p^n_{\mathcal{T}}\right]\!\right]_{\mathcal{T}} \leq \left\|q^{+,n}_{\mathcal{T}} - q^{-,n}_{\mathcal{T}}\right\|_{2,\mathcal{T}} \left\|p^n_{\mathcal{T}}\right\|_{2,\mathcal{T}} \tag{26}$$

Applying now the discrete Poincaré inequality (Theorem 3.1), we get simultaneously

$$\left\|\nabla^{\mathfrak{D}} p^n_{\mathcal{T}}\right\|_{2,\mathfrak{D}} \leq C \left\|q^{+,n}_{\mathcal{T}} - q^{-,n}_{\mathcal{T}}\right\|_{2,\mathcal{T}} \text{ and } \left\|p^n_{\mathcal{T}}\right\|_{2,\mathcal{T}} \leq C \left\|q^{+,n}_{\mathcal{T}} - q^{-,n}_{\mathcal{T}}\right\|_{2,\mathcal{T}} \forall 1 \leq n \leq N_T. \tag{27}$$

The relation (20) and the hypothesis (8) imply $\left\|\mathbf{U}^n_{\mathfrak{D}}\right\|_{2,\mathfrak{D}} \leq \Lambda_A \left\|\nabla^{\mathfrak{D}} p^n_{\mathcal{T}}\right\|_{2,\mathfrak{D}}$ and therefore

$$\left\|\mathbf{U}^n_{\mathfrak{D}}\right\|_{2,\mathfrak{D}} \leq C \|q^{+,n}_{\mathcal{T}} - q^{-,n}_{\mathcal{T}}\|_{2,\mathcal{T}} \forall 1 \leq n \leq N_T. \tag{28}$$

As

$$\max_{1\leq n\leq N_T} \left\|q^{+,n}_{\mathcal{T}} - q^{-,n}_{\mathcal{T}}\right\|_{2,\mathcal{T}} \leq \|q^+ - q^-\|_{L^\infty(0,T,L^2(\Omega))},$$

the estimate (25) is a consequence of (27) and (28).

□

Lemma 3.3 gives *a priori* estimates on the approximate concentration and its approximate gradient.

Lemma 3.3. *Let Ω be a convex polygonal domain of $\mathbb{R}^2$ and $\mathcal{T}$ a DDFV mesh of this domain. Assume* (7)–(12) *hold and that the scheme* (19)–(24) *has a solution $(p^n_{\mathcal{T}}, \mathbf{U}^n_{\mathfrak{D}}, c^n_{\mathcal{T}})_{1\leq n\leq N_T}$. Then, there exists $C > 0$ depending only on Ω, ζ, $\sin(\alpha_{\mathcal{T}})$, Φ^* and α_D, such that we have for all $N \in [1, \ldots, N_T]$:*

$$\left\|c^N_{\mathcal{T}}\right\|^2_{2,\mathcal{T}} + \sum_{n=1}^{N} \delta t \left\|\nabla^{\mathfrak{D}} c^n_{\mathcal{T}}\right\|^2_{2,\mathfrak{D}} + \sum_{n=1}^{N} \delta t \left\||\mathbf{U}^n_{\mathfrak{D}}|^{\frac{1}{2}} \nabla^{\mathfrak{D}} c^n_{\mathcal{T}}\right\|^2_{2,\mathfrak{D}} \leq C \left(\|c_0\|^2_{L^2(\Omega)} + \|q^+\|^2_{L^\infty(0,T,L^2(\Omega))}\right). \tag{29}$$

Proof. We multiply the scheme (23) by $c^n_{\mathcal{T}}$:

$$\left[\!\left[\Phi_{\mathcal{T}} \frac{c^n_{\mathcal{T}} - c^{n-1}_{\mathcal{T}}}{\delta t}, c^n_{\mathcal{T}}\right]\!\right]_{\mathcal{T}} - \left[\!\left[\mathrm{div}^{\mathcal{T}}\left(\mathbb{D}_{\mathfrak{D}}\left(\mathbf{U}^n_{\mathfrak{D}}\right)\nabla^{\mathfrak{D}} c^n_{\mathcal{T}}\right), c^n_{\mathcal{T}}\right]\!\right]_{\mathcal{T}} + \left[\!\left[\mathrm{divc}^{\mathcal{T}}\left(\mathbf{U}^n_{\mathfrak{D}}, c^n_{\mathcal{T}}\right), c^n_{\mathcal{T}}\right]\!\right]_{\mathcal{T}} + \left[\!\left[q^{-,n}_{\mathcal{T}} c^n_{\mathcal{T}}, c^n_{\mathcal{T}}\right]\!\right]_{\mathcal{T}}$$
$$= \left[\!\left[q^{+,n}_{\mathcal{T}} \hat{c}^n_{\mathcal{T}}, c^n_{\mathcal{T}}\right]\!\right]_{\mathcal{T}} \tag{30}$$

Let us analyse successively the different terms in this equality. The relation $(a-b)a = \frac{1}{2}(a^2-b^2) + \frac{1}{2}(a-b)^2$ ensures

$$\left[\!\left[\Phi_{\mathcal{T}}(c^n_{\mathcal{T}} - c^{n-1}_{\mathcal{T}}), c^n_{\mathcal{T}}\right]\!\right]_{\mathcal{T}} \geq \frac{1}{2}\left(\left[\!\left[\Phi_{\mathcal{T}}, (c^n_{\mathcal{T}})^2\right]\!\right]_{\mathcal{T}} - \left[\!\left[\Phi_{\mathcal{T}}, (c^{n-1}_{\mathcal{T}})^2\right]\!\right]_{\mathcal{T}}\right)$$

Thanks to the Neumann boundary conditions (24), Theorem 2.3 and hypothesis (9) lead to:

$$-\left[\!\left[\mathrm{div}^{\mathcal{T}}\left(\mathbb{D}_{\mathfrak{D}}\left(\mathbf{U}^n_{\mathfrak{D}}\right)\nabla^{\mathfrak{D}} c^n_{\mathcal{T}}\right), c^n_{\mathcal{T}}\right]\!\right]_{\mathcal{T}} = \quad \left(\mathbb{D}_{\mathfrak{D}}\left(\mathbf{U}^n_{\mathfrak{D}}\right)\nabla^{\mathfrak{D}} c^n_{\mathcal{T}}, \nabla^{\mathfrak{D}} c^n_{\mathcal{T}}\right)_{\mathfrak{D}}$$
$$\geq \quad \alpha_D\left(\left\|\nabla^{\mathfrak{D}} c^n_{\mathcal{T}}\right\|^2_{2,\mathfrak{D}} + \left\||\mathbf{U}^n_{\mathfrak{D}}|^{\frac{1}{2}} \nabla^{\mathfrak{D}} c^n_{\mathcal{T}}\right\|^2_{2,\mathfrak{D}}\right).$$

Due to the boundary conditions (21), Lemma 2.5 and (19) imply:

$$\left[\!\left[\mathrm{divc}^{\mathcal{T}}\left(\mathbf{U}^n_{\mathfrak{D}}, c^n_{\mathcal{T}}\right), c^n_{\mathcal{T}}\right]\!\right]_{\mathcal{T}} \geq \frac{1}{2}\left[\!\left[\mathrm{div}^{\mathcal{T}}(\mathbf{U}^n_{\mathfrak{D}}), \left(c^n_{\mathcal{T}}\right)^2\right]\!\right]_{\mathcal{T}} \geq \frac{1}{2}\left[\!\left[q^{+,n}_{\mathcal{T}} - q^{-,n}_{\mathcal{T}}, \left(c^n_{\mathcal{T}}\right)^2\right]\!\right]_{\mathcal{T}}$$

and, as $[\![q_{\mathcal{T}}^{-,n} c_{\mathcal{T}}^n, c_{\mathcal{T}}^n]\!]_{\mathcal{T}} = \left[\!\left[q_{\mathcal{T}}^{-,n}, \left(c_{\mathcal{T}}^n\right)^2\right]\!\right]_{\mathcal{T}}$, we obtain:

$$\left[\!\left[\mathrm{divc}^{\mathcal{T}}\left(\mathbf{U}_{\mathfrak{D}}^n, c_{\mathcal{T}}^n\right), c_{\mathcal{T}}^n\right]\!\right]_{\mathcal{T}} + [\![q_{\mathcal{T}}^{-,n} c_{\mathcal{T}}^n, c_{\mathcal{T}}^n]\!]_{\mathcal{T}} \geq \frac{1}{2}\left[\!\left[q_{\mathcal{T}}^{+,n} + q_{\mathcal{T}}^{-,n}, \left(c_{\mathcal{T}}^n\right)^2\right]\!\right]_{\mathcal{T}} \geq 0.$$

Finally, thanks to Cauchy-Schwarz inequality and hypotheses (11) , we have

$$[\![q_{\mathcal{T}}^{+,n} \hat{c}_{\mathcal{T}}^n, c_{\mathcal{T}}^n]\!]_{\mathcal{T}} \leq \left\|q_{\mathcal{T}}^{+,n} \hat{c}_{\mathcal{T}}^n\right\|_{2,\mathcal{T}} \left\|c_{\mathcal{T}}^n\right\|_{2,\mathcal{T}} \leq \left\|q_{\mathcal{T}}^{+,n}\right\|_{2,\mathcal{T}} \left\|c_{\mathcal{T}}^n\right\|_{2,\mathcal{T}}.$$

Therefore, from equality (30), we get:

$$\frac{1}{2\delta t}\left([\![\Phi_{\mathcal{T}}, (c_{\mathcal{T}}^n)^2]\!]_{\mathcal{T}} - [\![\Phi_{\mathcal{T}}, (c_{\mathcal{T}}^{n-1})^2]\!]_{\mathcal{T}}\right) + \alpha_D\left(\left\|\nabla^{\mathfrak{D}} c_{\mathcal{T}}^n\right\|_{2,\mathfrak{D}}^2 + \left\||\mathbf{U}_{\mathfrak{D}}^n|^{\frac{1}{2}} \nabla^{\mathfrak{D}} c_{\mathcal{T}}^n\right\|_{2,\mathfrak{D}}^2\right) \leq \left\|q_{\mathcal{T}}^{+,n}\right\|_{2,\mathcal{T}} \left\|c_{\mathcal{T}}^n\right\|_{2,\mathcal{T}}. \tag{31}$$

Multiplying by $2\delta t$ and summing over $n = 1, \ldots, N$ with $1 \leq N \leq N_T$, we get

$$[\![\Phi_{\mathcal{T}}, (c_{\mathcal{T}}^N)^2]\!]_{\mathcal{T}} - [\![\Phi_{\mathcal{T}}, (c_{\mathcal{T}}^0)^2]\!]_{\mathcal{T}} + 2\alpha_D \sum_{n=1}^N \delta t\left(\left\|\nabla^{\mathfrak{D}} c_{\mathcal{T}}^n\right\|_{2,\mathfrak{D}}^2 + \left\||\mathbf{U}_{\mathfrak{D}}^n|^{\frac{1}{2}} \nabla^{\mathfrak{D}} c_{\mathcal{T}}^n\right\|_{2,\mathfrak{D}}^2\right) \leq 2\sum_{n=1}^N \delta t \left\|q_{\mathcal{T}}^{+,n}\right\|_{2,\mathcal{T}} \left\|c_{\mathcal{T}}^n\right\|_{2,\mathcal{T}}. \tag{32}$$

But, the hypotheses on Φ (10) ensure:

$$\begin{array}{rcl} [\![\Phi_{\mathcal{T}}, (c_{\mathcal{T}}^N)^2]\!]_{\mathcal{T}} & \geq & \Phi_* \|c_{\mathcal{T}}^N\|_{2,\mathcal{T}}^2 \\ [\![\Phi_{\mathcal{T}}, (c_{\mathcal{T}}^0)^2]\!]_{\mathcal{T}} & \leq & \Phi_*^{-1} \|c_{\mathcal{T}}^0\|_{2,\mathcal{T}}^2 \leq \Phi_*^{-1} \|c_0\|_{L^2(\Omega)}^2. \end{array}$$

For the right-hand side in (32), we have:

$$\begin{array}{rcl} \displaystyle\sum_{n=1}^N \delta t \left\|q_{\mathcal{T}}^{+,n}\right\|_{2,\mathcal{T}} \left\|c_{\mathcal{T}}^n\right\|_{2,\mathcal{T}} & \leq & T\|q^+\|_{L^\infty(0,T,L^2(\Omega))} \displaystyle\sup_{n\in[1,\ldots,N_T]} \|c_{\mathcal{T}}^n\|_{2,\mathcal{T}} \\ & \leq & \dfrac{T^2}{\Phi_*}\|q^+\|_{L^\infty(0,T,L^2(\Omega))}^2 + \dfrac{\Phi_*}{4} \displaystyle\sup_{n\in[1,\ldots,N_T]} \|c_{\mathcal{T}}^n\|_{2,\mathcal{T}}^2. \end{array}$$

Therefore, we deduce from (32) that, for all $N \in [1, \ldots, N_T]$,

$$\begin{array}{l} \Phi_* \|c_{\mathcal{T}}^N\|_{2,\mathcal{T}}^2 + 2\alpha_D \displaystyle\sum_{n=1}^N \delta t\left(\left\|\nabla^{\mathfrak{D}} c_{\mathcal{T}}^n\right\|_{2,\mathfrak{D}}^2 + \left\||\mathbf{U}_{\mathfrak{D}}^n|^{\frac{1}{2}} \nabla^{\mathfrak{D}} c_{\mathcal{T}}^n\right\|_{2,\mathfrak{D}}^2\right) \\ \qquad \leq \Phi_*^{-1}\|c_0\|_{L^2(\Omega)}^2 + \dfrac{2T^2C^2}{\Phi_*}\|q^+\|_{L^\infty(0,T,L^2(\Omega))}^2 + \dfrac{\Phi_*}{2} \displaystyle\sup_{n\in[1,\ldots,N_T]} \|c_{\mathcal{T}}^n\|_{2,\mathcal{T}}^2. \end{array}$$

We first focus on the term $\Phi_*\|c_{\mathcal{T}}^N\|_{2,\mathcal{T}}^2$ of the left hand side of the previous inequality, which is bounded by the right hand side. Taking now the supremum over $N \in [1, \ldots, N_T]$ yields the expected inequality (29) of this term. Finally, for the other terms of the left hand side of the previous inequality, we directly have the expected inequality (29).

□

3.2. Existence and uniqueness of an approximate solution

In this Section, we prove Theorem 3.4. It consists in the proof of invertibility of the two linear systems (19)–(22) and (23)-(24) involved at each time step.

Theorem 3.4. *Let Ω be a convex polygonal domain of $\mathbb{R}^2$ and $\mathcal{T}$ a DDFV mesh of this domain. Assume* (7)–(12) *hold. Let $T > 0$ and δt be a time step such that $N_T = T/\delta t$ is an integer. Then, the scheme* (19)–(24) *admits a unique solution $(p_{\mathcal{T}}^n, \mathbf{U}_{\mathfrak{D}}^n, c_{\mathcal{T}}^n)_{1\leq n\leq N_T}$.*

Step 1: Existence and uniqueness of $(p_{\mathcal{T}}^n, \mathbf{U}_{\mathfrak{D}}^n)$

Let us first consider the system (19)–(22) on $(p_{\mathcal{T}}^n, \mathbf{U}_{\mathfrak{D}}^n)$. The number of unknowns of the system is $\mathrm{Card}(\mathfrak{M}) + \mathrm{Card}(\partial\mathfrak{M}) + \mathrm{Card}(\mathfrak{M}^*) + \mathrm{Card}(\partial\mathfrak{M}^*) + \mathrm{Card}(\mathfrak{D})$. Equations (19), (20) and (21) provide respectively $\mathrm{Card}(\mathfrak{M}) + \mathrm{Card}(\mathfrak{M}^*) + \mathrm{Card}(\partial\mathfrak{M}^*)$, $\mathrm{Card}(\mathfrak{D})$ and $\mathrm{Card}(\mathfrak{D}_{ext})$ equations. As $\mathrm{Card}(\mathfrak{D}_{ext}) = \mathrm{Card}(\partial\mathfrak{M})$, the system (19)–(21) is a square system.

Inequality (26) gives us the kernel of this square system. Indeed, $q_{\mathcal{T}}^{+,n} - q_{\mathcal{T}}^{-,n} = 0$ implies $\nabla^{\mathfrak{D}} p_{\mathcal{T}}^n = 0$ and, thanks to the definition of the discrete gradient (2.1),

$$\nabla^{\mathfrak{D}} p_{\mathcal{T}}^n = 0 \Longleftrightarrow p_{\mathcal{K}}^n = P,\ \forall \mathcal{K} \in \overline{\mathfrak{M}} \text{ and } p_{\mathcal{K}^*}^n = \widetilde{P},\ \forall \mathcal{K}^* \in \overline{\mathfrak{M}^*}.$$

Therefore, the kernel of the square system (19)–(21) has dimension 2. Let us now multiply the scheme (19) by the test function $v_{\mathcal{T}}$ defined by $v_{\mathcal{K}} = 1$ for all $\mathcal{K} \in \overline{\mathfrak{M}}$ and $v_{\mathcal{K}^*} = 0$ for all $\mathcal{K}^* \in \overline{\mathfrak{M}^*}$. We obtain :

$$\sum_{\mathcal{K}\in\mathfrak{M}} \mathrm{m}_{\mathcal{K}}(q_{\mathcal{K}}^{+,n} - q_{\mathcal{K}}^{-,n}) = \left[\!\left[q_{\mathcal{T}}^{+,n} - q_{\mathcal{T}}^{-,n}, v_{\mathcal{T}} \right]\!\right]_{\mathcal{T}} = \left[\!\left[\mathrm{div}^{\mathcal{T}}(\mathbf{U}_{\mathfrak{D}}^n), v_{\mathcal{T}} \right]\!\right]_{\mathcal{T}} = -(\mathbf{U}_{\mathfrak{D}}^n, \nabla^{\mathfrak{D}} v_{\mathcal{T}})_{\mathfrak{D}} = 0.$$

With the test function $w_{\mathcal{T}}$ defined by $w_{\mathcal{K}} = 0$ for all $\mathcal{K} \in \overline{\mathfrak{M}}$ and $w_{\mathcal{K}^*} = 0$ for all $\mathcal{K}^* \in \overline{\mathfrak{M}^*}$, we get similarly

$$\sum_{\mathcal{K}^*\in\overline{\mathfrak{M}^*}} \mathrm{m}_{\mathcal{K}^*}(q_{\mathcal{K}^*}^{+,n} - q_{\mathcal{K}^*}^{-,n}) = \left[\!\left[q_{\mathcal{T}}^{+,n} - q_{\mathcal{T}}^{-,n}, w_{\mathcal{T}} \right]\!\right]_{\mathcal{T}} = 0.$$

The relations $\sum_{\mathcal{K}\in\mathfrak{M}} \mathrm{m}_{\mathcal{K}}(q_{\mathcal{K}}^{+,n} - q_{\mathcal{K}}^{-,n}) = 0$ and $\sum_{\mathcal{K}^*\in\overline{\mathfrak{M}^*}} \mathrm{m}_{\mathcal{K}^*}(q_{\mathcal{K}^*}^{+,n} - q_{\mathcal{K}^*}^{-,n}) = 0$ ensure that the right hand-side of the linear system belongs to the image of the matrix of the system. As these conditions are satisfied, thanks to hypothesis (7), the system (19)–(22) is invertible. Its solutions are not unique: they are defined up to the constants P and $\widetilde{P}$. But, the values of P and $\widetilde{P}$ are fixed by (22). Therefore, the system (19)–(22) admits a unique solution.

Step 2: Existence and uniqueness of $c_{\mathcal{T}}^n$

We now consider the system (23)-(24) on $c_{\mathcal{T}}^n$. The number of unknowns is $\mathrm{Card}(\mathfrak{M}) + \mathrm{Card}(\partial\mathfrak{M}) + \mathrm{Card}(\mathfrak{M}^*) + \mathrm{Card}(\partial\mathfrak{M}^*)$, equal to the number of equations. Inequality (31) written with $c_{\mathcal{T}}^{n-1} = 0$ and $q_{\mathcal{T}}^{+,n} = 0$ imply that the kernel of the linear system is reduced to 0. Therefore, there exists a unique $c_{\mathcal{T}}^n$ solution to (23)-(24).

It concludes the proof of Theorem 3.4.

4. Numerical convergence of the DDFV scheme

In this section, we illustrate the behavior of DDFV scheme by applying it to the system (1)—(3), which describes the miscible displacement of one fluid by another in a porous medium.

In all the test cases, the spatial domain is $\Omega = (0, 1000) \times (0, 1000)$ ft^2 and the time period is $[0, 3600]$ days. The injection well is located at the upper-right corner $(1000, 1000)$ with an injection rate $q^+ = 30$ ft^2/day and an injection concentration $\hat{c} = 1.0$. The production well is located at the lower-left corner $(0, 0)$ with a production rate $q^- = 30$ ft^2/day. It means that q^- and q^+ are Dirac masses, which can be taken into account with the scheme. The porosity of the medium is specified as $\Phi(x) = 0.1$ and the initial concentration is $c_0(x) = 0$. The viscosity of the oil is $\mu(0)$=1.0 cp. We choose $\Phi d_l = 5$ ft and $\Phi d_t = 0.5$ ft.

In order to compute the numerical order of convergence of the scheme, we introduce a sequence of triangular meshes. For a refinement level $i \in \{1, \cdots, 7\}$, the mesh is obtained by dividing the domain into $2^{i+1} \times 2^{i+1}$ equally sized squares and each square is split into 2 triangles along a diagonal. The number of cells for the mesh i is 2^{2i+3}. We present on Figure 4.1 the meshes obtained for $i = 1$ and $i = 3$.

We take as the reference solution the solution computed on the mesh $i = 7$ and we compute the relative errors in L^1-norm and L^2-norm at time $T = 3600$ days. The time step is $\delta t = 36$ days.

Test 1: In this test case, we assume that the viscosity is constant, $\mu(c) = 1$ cp. And we set $\Phi d_m = 1$ ft^2/day. We compare the results obtained for two different values of the permeability : a constant one $\mathbb{K} = 80\,\mathbb{I}$ and a discontinuous one $\mathbb{K} = 80\,\mathbb{I}$ on the subdomain $(0, 1000) \times (0, 500)$ and $\mathbb{K} = 20\,\mathbb{I}$ on the subdomain $(0, 1000) \times (500, 1000)$.

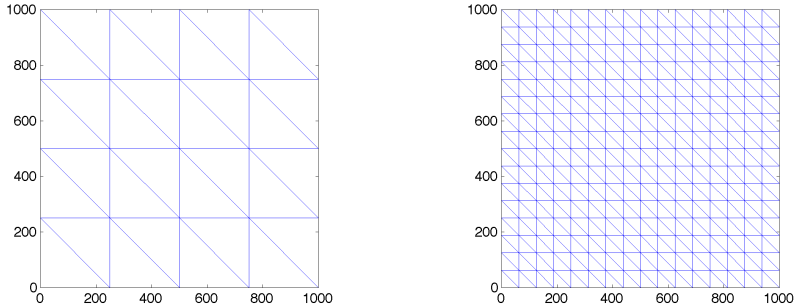

Figure 4.1: Triangular meshes with a refinement level $i = 1$ on the left and $i = 3$ on the right.

In Table 4.1, we first compare the L^1-norm and L^2-norm of the pressure error. When the permeability $\mathbb{K}$ is continuous, we observe a order of convergence in L^1-norm around 2 while it is only less than 1.2 in L^2-norm. When the permeability $\mathbb{K}$ is discontinuous, we note that the values of the errors in L^1-norm and L^2-norm are close and the order of convergence in L^1-norm is now around 1.2. In fact, this loss of convergence has already been observed by Boyer-Hubert in [8].

refinement	$\mathbb{K} = 80\,\mathbb{I}$				$\mathbb{K} = (80\mathbf{1}_{y<500} + 20\mathbf{1}_{y>500})\,\mathbb{I}$			
level	error L^1	order L^1	error L^2	order L^2	error L^1	order L^1	error L^2	order L^2
1	2.72e-02	-	5.15e-02	-	1.63e-01	-	1.30e-01	-
2	7.57e-03	2.14	2.50e-02	1.18	7.95e-02	1.19	6.20e-02	1.21
3	2.21e-03	1.93	1.24e-02	1.09	3.83e-02	1.14	2.98e-02	1.13
4	6.35e-04	1.88	6.18e-03	1.05	1.78e-02	1.15	1.41e-02	1.13
5	1.74e-04	1.91	3.02e-03	1.06	7.64e-03	1.25	6.26e-03	1.19
6	4.08e-05	2.12	1.32e-03	1.21	2.55e-03	1.60	2.31e-03	1.46

Table 4.1: Test 1. Convergence results of the DDFV method on the pressure p at time $t = 3600$.

In Table 4.2, we compare the different orders of convergence for the concentration. We observe the same kind of results : order around 1, in L^1-norm as in L^2-norm, for the continuous permeability and the discontinuous one.

Let us just mention that we obtain similar results using a sequence of square meshes.

Test 2 : In this test case, we assume that the viscosity really depends on c and is given by (4) with $M = 41$. The dependence on c of the viscosity induces a strong coupling in the system. We also assume that there is no molecular diffusion $\Phi d_m = 0$ ft^2/day. We still compare the results obtained for two different values of the permeability : a constant one $\mathbb{K} = 80\,\mathbb{I}$ and a discontinuous one $\mathbb{K} = 80\,\mathbb{I}$ on the subdomain $(0, 1000) \times (0, 500)$ and $\mathbb{K} = 20\,\mathbb{I}$ on the

refinement	$\mathbb{K} = 80\,\mathbb{I}$				$\mathbb{K} = (80\mathbf{1}_{y<500} + 20\mathbf{1}_{y>500})\,\mathbb{I}$			
level	error L^1	order L^1	error L^2	order L^2	error L^1	order L^1	error L^2	order L^2
1	4.66e-02	-	6.13e-02	-	4.60e-02	-	6.02e-02	-
2	3.28e-02	0.58	4.49e-02	0.52	3.26e-02	0.57	4.53e-02	0.47
3	2.03e-02	0.75	2.84e-02	0.72	2.02e-02	0.75	2.88e-02	0.71
4	1.11e-02	0.91	1.58e-02	0.89	1.10e-02	0.92	1.60e-02	0.88
5	5.20e-03	1.12	7.52e-03	1.09	5.13e-03	1.12	7.66e-03	1.09
6	1.83e-03	1.53	2.67e-03	1.51	1.80e-03	1.53	2.73e-03	1.51

Table 4.2: Test 1. Convergence results of the DDFV method on the concentration c at time $t = 3600$.

subdomain $(0, 1000) \times (500, 1000)$.

In Tables 4.3 and 4.4, we compare the different orders of convergence for the pressure and the concentration. We observe a loss of accuracy for both variables and both values of permeability. Especially we remark that for a continuous permeability we do not preserve the order 2 for the pressure.

refinement	$\mathbb{K} = 80\,\mathbb{I}$		$\mathbb{K} = (80\mathbf{1}_{y<500} + 20\mathbf{1}_{y>500})\,\mathbb{I}$	
level	error L^1	order L^1	error L^1	order L^1
1	2.78e-01	-	3.71e-01	-
2	2.95e-01	-0.12	2.65e-01	0.56
3	2.67e-01	0.15	1.73e-01	0.66
4	1.95e-01	0.47	1.18e-01	0.57
5	1.01e-01	0.97	7.17e-02	0.74
6	3.49e-02	1.55	3.45e-02	1.07

Table 4.3: Test2. Convergence results of the DDFV method on the pressure p at time $t = 3600$.

refinement	$\mathbb{K} = 80\,\mathbb{I}$		$\mathbb{K} = (80\mathbf{1}_{y<500} + 20\mathbf{1}_{y>500})\,\mathbb{I}$	
level	error L^1	order L^1	error L^1	order L^1
1	4.96e-01	-	4.69e-01	-
2	4.11e-01	0.31	3.67e-01	0.41
3	3.19e-01	0.40	2.62e-01	0.53
4	2.19e-01	0.56	1.68e-01	0.67
5	1.22e-01	0.87	9.44e-02	0.85
6	4.80e-02	1.36	4.16e-02	1.20

Table 4.4: Test 2. Convergence results of the DDFV method on the concentration c at time $t = 3600$.

5. An other scheme: the m-DDFV scheme

As shown in Table 4.1 the DDFV scheme for anisotropic diffusion equation has order 2 in the case where the diffusion tensor is continuous but only order 1 when it is discontinuous. It has already been observed in [8], and therefore these authors introduce a new DDFV scheme called m-DDFV.

In this part, we focus on a diffusive tensor $\mathbb{A}(x, c) = \frac{\mathbb{K}(x)}{\mu(c)}$ such that $\mathbb{K}$ is discontinuous across the primal edges. In [26, 8], the authors have proposed to modify the discrete gradient and the numerical fluxes in order to recover a scheme of order one. Note that in [8] the tensor is more general and it is discontinuous across primal and dual edges. First we recall the idea and the definition of the discrete gradient. Then in Section 5.3, we apply this method to our problem (5)-(6).

5.1. Notations

In this section, we need to introduce additional notations, as shown on Figure 5.1. For any $\mathcal{D} \in \mathfrak{D}$, we define the half-diamonds $\widetilde{\mathcal{D}}_\mathcal{K} = \mathcal{D} \cap \mathcal{K}$ and $\widetilde{\mathcal{D}}_\mathcal{L} = \mathcal{D} \cap \mathcal{L}$, such that $\mathcal{D} = \widetilde{\mathcal{D}}_\mathcal{K} \cup \widetilde{\mathcal{D}}_\mathcal{L}$ if $\mathcal{D} \in \mathfrak{D}_{int}$ and $\mathcal{D} = \widetilde{\mathcal{D}}_\mathcal{K}$ if $\mathcal{D} \in \mathfrak{D}_{ext}$. A half-diamond is denoted by $\widetilde{\mathcal{D}}$ and the set of all the half-diamonds of the mesh is denoted by $\widetilde{\mathfrak{D}}$. For any $\mathcal{D} \in \mathfrak{D}$, we recall that $x_\mathcal{D}$ is the center of $\mathcal{D}$ and we introduce the half-edges $\sigma_\mathcal{K} = [x_\mathcal{K}, x_\mathcal{D}]$ and $\sigma_\mathcal{L} = [x_\mathcal{L}, x_\mathcal{D}]$, such that $\sigma = \sigma_\mathcal{K} \cup \sigma_\mathcal{L}$. Then, $\mathrm{m}_{\sigma_\mathcal{K}}$ denotes the measure of $\sigma_\mathcal{K}$ and $x_{\sigma_\mathcal{K}}$ its center (and we define similarly $\mathrm{m}_{\sigma_\mathcal{L}}$ and $x_{\sigma_\mathcal{L}}$).

We consider the linear spaces $\left(\mathbb{R}^2\right)^{\widetilde{\mathfrak{D}}}$ of vector fields constant on the cells of $\widetilde{\mathfrak{D}}$:

$$\left(\mathbb{R}^2\right)^{\widetilde{\mathfrak{D}}} = \left\{\boldsymbol{\xi}_{\widetilde{\mathfrak{D}}} = \left(\boldsymbol{\xi}_{\widetilde{\mathcal{D}}}\right)_{\widetilde{\mathcal{D}} \in \widetilde{\mathfrak{D}}},\ \text{with } \boldsymbol{\xi}_{\widetilde{\mathcal{D}}} \in \mathbb{R}^2,\ \forall \widetilde{\mathcal{D}} \in \widetilde{\mathfrak{D}}\right\}.$$

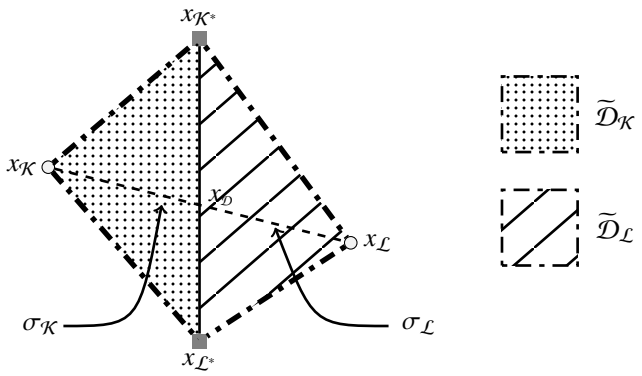

Figure 5.1: A diamond $\mathcal{D}$ with the half-diamonds $\widetilde{\mathcal{D}}_{\mathcal{K}}$ and $\widetilde{\mathcal{D}}_{\mathcal{L}}$.

We also define an added scalar product $(\cdot,\cdot)_{\widetilde{\mathfrak{D}}}$ on $\left(\mathbb{R}^2\right)^{\widetilde{\mathfrak{D}}}$ by

$$\left(\boldsymbol{\xi}_{\widetilde{\mathfrak{D}}}, \boldsymbol{\varphi}_{\widetilde{\mathfrak{D}}}\right)_{\widetilde{\mathfrak{D}}} = \sum_{\tilde{\mathcal{D}}\in\widetilde{\mathfrak{D}}} m_{\tilde{\mathcal{D}}}\, \boldsymbol{\xi}_{\widetilde{\mathcal{D}}} \cdot \boldsymbol{\varphi}_{\widetilde{\mathcal{D}}}, \quad \forall \boldsymbol{\xi}_{\widetilde{\mathfrak{D}}}, \boldsymbol{\varphi}_{\widetilde{\mathfrak{D}}} \in \left(\mathbb{R}^2\right)^{\widetilde{\mathfrak{D}}},$$

the corresponding norm is denoted by $\|\cdot\|_{2,\widetilde{\mathfrak{D}}}$:

$$\left\|\boldsymbol{\xi}_{\widetilde{\mathfrak{D}}}\right\|_{2,\widetilde{\mathfrak{D}}} = \left(\sum_{\tilde{\mathcal{D}}\in\widetilde{\mathfrak{D}}} m_{\tilde{\mathcal{D}}}\, |\boldsymbol{\xi}_{\widetilde{\mathcal{D}}}|^2\right)^{1/2}, \quad \forall \boldsymbol{\xi}_{\widetilde{\mathfrak{D}}} \in \left(\mathbb{R}^2\right)^{\widetilde{\mathfrak{D}}}.$$

5.2. The modified discrete gradient

When the anisotropic tensor $\mathbb{K}$ is discontinuous across the primal edges, the normal component of $\mathbb{K}\nabla u$ must be continuous across these primal edges. For instance, we have for $\sigma = \mathcal{K}|\mathcal{L} = \widetilde{\mathcal{D}}_{\mathcal{K}}|\widetilde{\mathcal{D}}_{\mathcal{L}}$

$$\int_{\sigma} \left(\mathbb{K}_{|\widetilde{\mathcal{D}}_{\mathcal{K}}} \nabla u_{|\widetilde{\mathcal{D}}_{\mathcal{K}}}\right) \cdot \mathbf{n}_{\sigma\mathcal{K}} \mathrm{d}s = \int_{\sigma} \left(\mathbb{K}_{|\widetilde{\mathcal{D}}_{\mathcal{L}}} \nabla u_{|\widetilde{\mathcal{D}}_{\mathcal{L}}}\right) \cdot \mathbf{n}_{\sigma\mathcal{K}} \mathrm{d}s.$$

We need to impose this consistance at the discret level. Therefore, we introduce a new discrete gradient $\nabla^{\widetilde{\mathfrak{D}}}$, piecewise constant on the half-diamonds. In the definition of this new discrete gradient, we introduce new unknowns u_σ which will be algebrically eliminated in the sequel.

Definition 5.1. *The discrete gradient $\nabla^{\widetilde{\mathfrak{D}}}$ is a mapping from $\mathbb{R}^{\mathcal{T}}$ to $\left(\mathbb{R}^2\right)^{\widetilde{\mathfrak{D}}}$ defined for all $u_{\mathcal{T}} \in \mathbb{R}^{\mathcal{T}}$ by $\nabla^{\widetilde{\mathfrak{D}}} u_{\mathcal{T}} = \left(\nabla^{\widetilde{\mathcal{D}}} u_{\mathcal{T}}\right)_{\tilde{\mathcal{D}}\in\widetilde{\mathfrak{D}}}$, where for $\widetilde{\mathcal{D}} \in \widetilde{\mathfrak{D}}$ whose vertices are $x_{\mathcal{K}}$, $x_{\mathcal{K}^*}$ and $x_{\mathcal{L}^*}$:*

$$\nabla^{\widetilde{\mathcal{D}}} u_{\mathcal{T}} = \frac{1}{\sin(\alpha_{\mathcal{D}})}\left(\frac{u_\sigma - u_{\mathcal{K}}}{\mathrm{m}_{\sigma_{\mathcal{K}}}}\mathbf{n}_{\sigma\mathcal{K}} + \frac{u_{\mathcal{L}^*} - u_{\mathcal{K}^*}}{\mathrm{m}_\sigma}\mathbf{n}_{\sigma^*\mathcal{K}^*}\right) \Longleftrightarrow \begin{cases} \nabla^{\widetilde{\mathcal{D}}} u_{\mathcal{T}} \cdot \boldsymbol{\tau}_{\mathcal{K}^*,\mathcal{L}^*} = & \dfrac{u_{\mathcal{L}^*} - u_{\mathcal{K}^*}}{\mathrm{m}_\sigma}, \\ \nabla^{\widetilde{\mathcal{D}}} u_{\mathcal{T}} \cdot \boldsymbol{\tau}_{\mathcal{K},\mathcal{L}} = & \dfrac{u_\sigma - u_{\mathcal{K}}}{\mathrm{m}_{\sigma_{\mathcal{K}}}}. \end{cases}$$

For any $\widetilde{\mathcal{D}} \in \widetilde{\mathfrak{D}}$, let us define by $\mathbb{K}_{\tilde{\mathcal{D}}}$ the mean value of $\mathbb{K}$ over $\widetilde{\mathcal{D}}$: $\mathbb{K}_{\tilde{\mathcal{D}}} = \dfrac{1}{m_{\tilde{\mathcal{D}}}}\displaystyle\int_{\tilde{\mathcal{D}}} \mathbb{K}(s)\mathrm{d}s$; $\mathbb{K}_{\tilde{\mathcal{D}}}$ is a definite positive matrix which approachs $\mathbb{K}$ on the half-diamond. To determine the unknowns u_σ, we impose, for all $\mathcal{D} = \mathcal{D}_{\sigma,\sigma^*} \in \mathfrak{D}_{int}$ such that $\mathcal{D} = \widetilde{\mathcal{D}}_{\mathcal{K}} \cup \widetilde{\mathcal{D}}_{\mathcal{L}}$, the following condition:

$$(\mathbb{K}_{\tilde{\mathcal{D}}_{\mathcal{K}}} \nabla^{\widetilde{\mathcal{D}}_{\mathcal{K}}} u_{\mathcal{T}}) \cdot \mathbf{n}_{\sigma\mathcal{K}} = (\mathbb{K}_{\tilde{\mathcal{D}}_{\mathcal{L}}} \nabla^{\widetilde{\mathcal{D}}_{\mathcal{L}}} u_{\mathcal{T}}) \cdot \mathbf{n}_{\sigma\mathcal{K}}, \tag{33}$$

Furthermore, for all $\mathcal{D}_{\sigma,\sigma^*} \in \mathfrak{D}_{ext}$ we take $u_\sigma = u_{\mathcal{L}}$. We remark that on the boundary the diamond $\mathcal{D} \in \mathfrak{D}_{ext}$ coincide with the half-diamond $\widetilde{\mathcal{D}}$ and therefore $\nabla^{\mathcal{D}} u_{\mathcal{T}} = \nabla^{\widetilde{\mathcal{D}}} u_{\mathcal{T}}$.

Proposition 5.2. *Let $u_{\mathcal{T}} \in \mathbb{R}^{\mathcal{T}}$. For all $\mathcal{D}_{\sigma,\sigma^*} \in \mathfrak{D}_{int}$, there exists a unique u_σ solution to* (33)*:*

$$\begin{aligned} u_\sigma = \frac{\mathrm{m}_{\sigma_\mathcal{K}}\mathrm{m}_{\sigma_\mathcal{L}}}{\Big((\mathbb{K}_{\tilde{\mathcal{D}}_\mathcal{K}}\mathrm{m}_{\sigma_\mathcal{L}} + \mathbb{K}_{\tilde{\mathcal{D}}_\mathcal{L}}\mathrm{m}_{\sigma_\mathcal{K}})\mathbf{n}_{\sigma\mathcal{K}}\Big)\cdot\mathbf{n}_{\sigma\mathcal{K}}}\Big[u_\mathcal{K}\frac{(\mathbb{K}_{\tilde{\mathcal{D}}_\mathcal{K}}\mathbf{n}_{\sigma\mathcal{K}})\cdot\mathbf{n}_{\sigma\mathcal{K}}}{\mathrm{m}_{\sigma_\mathcal{K}}} + u_\mathcal{L}\frac{(\mathbb{K}_{\tilde{\mathcal{D}}_\mathcal{L}}\mathbf{n}_{\sigma\mathcal{K}})\cdot\mathbf{n}_{\sigma\mathcal{K}}}{\mathrm{m}_{\sigma_\mathcal{L}}} \\ + \frac{u_{\mathcal{L}^*} - u_{\mathcal{K}^*}}{\mathrm{m}_\sigma}\Big(\Big(\mathbb{K}_{\tilde{\mathcal{D}}_\mathcal{L}} - \mathbb{K}_{\tilde{\mathcal{D}}_\mathcal{K}}\Big)\mathbf{n}_{\sigma^*\mathcal{K}^*}\Big)\cdot\mathbf{n}_{\sigma\mathcal{K}}\Big]. \end{aligned} \tag{34}$$

Proof. The relation (33) rewrites

$$\left(\left(\frac{\mathbb{K}_{\tilde{\mathcal{D}}_\mathcal{K}}}{\mathrm{m}_{\sigma_\mathcal{K}}} + \frac{\mathbb{K}_{\tilde{\mathcal{D}}_\mathcal{L}}}{\mathrm{m}_{\sigma_\mathcal{L}}}\right)\mathbf{n}_{\sigma\mathcal{K}}\right)\cdot\mathbf{n}_{\sigma\mathcal{K}}u_\sigma = u_\mathcal{K}\frac{(\mathbb{K}_{\tilde{\mathcal{D}}_\mathcal{K}}\mathbf{n}_{\sigma\mathcal{K}})\cdot\mathbf{n}_{\sigma\mathcal{K}}}{\mathrm{m}_{\sigma_\mathcal{K}}} + u_\mathcal{L}\frac{(\mathbb{K}_{\tilde{\mathcal{D}}_\mathcal{L}}\mathbf{n}_{\sigma\mathcal{K}})\cdot\mathbf{n}_{\sigma\mathcal{K}}}{\mathrm{m}_{\sigma_\mathcal{L}}} + \frac{u_{\mathcal{L}^*} - u_{\mathcal{K}^*}}{\mathrm{m}_\sigma}\Big(\Big(\mathbb{K}_{\tilde{\mathcal{D}}_\mathcal{L}} - \mathbb{K}_{\tilde{\mathcal{D}}_\mathcal{K}}\Big)\mathbf{n}_{\sigma^*\mathcal{K}^*}\Big)\cdot\mathbf{n}_{\sigma\mathcal{K}}.$$

Since the matrices $\mathbb{K}_{\tilde{\mathcal{D}}}$ are definite positive, the system is invertible and we get (34). □

Thanks to the discrete gradient on half-diamonds, we introduce new numerical velocities as follows.

Definition 5.3. *We define a mapping $\mathbf{K}^{\mathfrak{D}}$ from $\left(\mathbb{R}^2\right)^{\widetilde{\mathfrak{D}}}$ to $\left(\mathbb{R}^2\right)^{\mathfrak{D}}$ such that, for all $\boldsymbol{\xi}_{\widetilde{\mathfrak{D}}} \in \left(\mathbb{R}^2\right)^{\widetilde{\mathfrak{D}}}$,*

$$\begin{aligned} &\mathbf{K}^{\mathfrak{D}}(\boldsymbol{\xi}_{\widetilde{\mathfrak{D}}}) = \left(\mathbf{K}_\mathcal{D}(\boldsymbol{\xi}_{\widetilde{\mathfrak{D}}})\right)_{\mathcal{D}\in\mathfrak{D}}, \\ \text{where} \quad &\mathbf{K}_\mathcal{D}(\boldsymbol{\xi}_{\widetilde{\mathfrak{D}}}) = \frac{1}{\mathrm{m}_\mathcal{D}}\sum_{\tilde{\mathcal{D}}\in\widetilde{\mathfrak{D}}_\mathcal{D}} m_{\tilde{\mathcal{D}}}\mathbb{K}_{\tilde{\mathcal{D}}}\boldsymbol{\xi}_{\widetilde{\mathcal{D}}} \quad \forall\mathcal{D}\in\mathfrak{D}. \end{aligned}$$

Remark 5.4.

1. *if $\mathbb{K}$ is smooth on the whole domain, we can replace this definition by*

$$\mathbf{K}_\mathcal{D}(\boldsymbol{\xi}_{\widetilde{\mathfrak{D}}}) = \mathbb{K}(x_\mathcal{D})\boldsymbol{\xi}_\mathcal{D}, \forall\mathcal{D}\in\mathfrak{D}.$$

2. *If $\mathbb{K}$ is piecewise constant on the primal cells, with $\mathbb{K} = K_\mathcal{K}$ on the primal cell $\mathcal{K}$, we can rewrite $\mathbf{K}_\mathcal{D}(\boldsymbol{\xi}_{\widetilde{\mathfrak{D}}}) = \overline{K}_\mathcal{D}\boldsymbol{\xi}_\mathcal{D}$ where $\overline{K}_\mathcal{D}$ is defined by*

$$\begin{aligned} (\overline{K}_\mathcal{D}\mathbf{n}_{\sigma\mathcal{K}})\cdot\mathbf{n}_{\sigma\mathcal{K}} =& \frac{m_{\sigma^*}(K_\mathcal{K}\mathbf{n}_{\sigma\mathcal{K}})\cdot\mathbf{n}_{\sigma\mathcal{K}}(K_\mathcal{L}\mathbf{n}_{\sigma\mathcal{K}})\cdot\mathbf{n}_{\sigma\mathcal{K}}}{\mathrm{m}_{\sigma_\mathcal{L}}(K_\mathcal{K}\mathbf{n}_{\sigma\mathcal{K}})\cdot\mathbf{n}_{\sigma\mathcal{K}} + \mathrm{m}_{\sigma_\mathcal{K}}(K_\mathcal{L}\mathbf{n}_{\sigma\mathcal{K}})\cdot\mathbf{n}_{\sigma\mathcal{K}}}, \\ (\overline{K}_\mathcal{D}\mathbf{n}_{\sigma^*\mathcal{K}^*})\cdot\mathbf{n}_{\sigma^*\mathcal{K}^*} =& \frac{\mathrm{m}_{\sigma_\mathcal{L}}(K_\mathcal{L}\mathbf{n}_{\sigma^*\mathcal{K}^*})\cdot\mathbf{n}_{\sigma^*\mathcal{K}^*} + \mathrm{m}_{\sigma_\mathcal{K}}(K_\mathcal{K}\mathbf{n}_{\sigma^*\mathcal{K}^*},\mathbf{n}_{\sigma^*\mathcal{K}^*})}{m_{\sigma^*}} \\ &- \frac{\mathrm{m}_{\sigma_\mathcal{K}}\mathrm{m}_{\sigma_\mathcal{L}}}{m_{\sigma^*}}\frac{((K_\mathcal{K}\mathbf{n}_{\sigma\mathcal{K}})\cdot\mathbf{n}_{\sigma^*\mathcal{K}^*} - (K_\mathcal{L}\mathbf{n}_{\sigma\mathcal{K}})\cdot\mathbf{n}_{\sigma^*\mathcal{K}^*})^2}{\mathrm{m}_{\sigma_\mathcal{L}}(K_\mathcal{K}\mathbf{n}_{\sigma\mathcal{K}})\cdot\mathbf{n}_{\sigma\mathcal{K}} + \mathrm{m}_{\sigma_\mathcal{K}}(K_\mathcal{L}\mathbf{n}_{\sigma\mathcal{K}})\cdot\mathbf{n}_{\sigma\mathcal{K}}}, \\ (\overline{K}_\mathcal{D}\mathbf{n}_{\sigma\mathcal{K}})\cdot\mathbf{n}_{\sigma^*\mathcal{K}^*} =& \frac{\mathrm{m}_{\sigma_\mathcal{L}}(K_\mathcal{L}\mathbf{n}_{\sigma\mathcal{K}})\cdot\mathbf{n}_{\sigma^*\mathcal{K}^*}(K_\mathcal{K}\mathbf{n}_{\sigma\mathcal{K}})\cdot\mathbf{n}_{\sigma\mathcal{K}} + \mathrm{m}_{\sigma_\mathcal{K}}(K_\mathcal{K}\mathbf{n}_{\sigma\mathcal{K}})\cdot\mathbf{n}_{\sigma^*\mathcal{K}^*}(K_\mathcal{L}\mathbf{n}_{\sigma\mathcal{K}})\cdot\mathbf{n}_{\sigma\mathcal{K}}}{\mathrm{m}_{\sigma_\mathcal{L}}(K_\mathcal{K}\mathbf{n}_{\sigma\mathcal{K}})\cdot\mathbf{n}_{\sigma\mathcal{K}} + \mathrm{m}_{\sigma_\mathcal{K}}(K_\mathcal{L}\mathbf{n}_{\sigma\mathcal{K}})\cdot\mathbf{n}_{\sigma\mathcal{K}}}. \end{aligned} \tag{35}$$

3. *Each interior diamond $\mathcal{D}$, whose vertices are $x_\mathcal{K}$, $x_{\mathcal{K}^*}$, $x_\mathcal{L}$, $x_{\mathcal{L}^*}$ and whose center is $x_\mathcal{D}$, can be splitted into four triangles $(x_\mathcal{K}x_{\mathcal{K}^*}x_\mathcal{D})$, $(x_{\mathcal{K}^*}x_\mathcal{L}x_\mathcal{D})$, $(x_\mathcal{L}x_{\mathcal{L}^*}x_\mathcal{D})$ and $(x_{\mathcal{L}^*}x_\mathcal{K}x_\mathcal{D})$ which can be called "quarter diamond cells". In [8], the diffusive tensor $\mathbb{K}$ is assumed to be smooth only on the quarter diamond cells and the discrete gradient operator is defined as piecewise constant on the quarter diamond cells. In the case where the diffusive tensor is only discontinuous across primal edges and then smooth on half-diamonds, the discrete gradient operator introduced here coincides with the discrete gradient operator defined in [8].*

5.3. The m-DDFV scheme

In this section, we give the modified DDFV scheme called m-DDFV scheme. It differs from (19)-(24) in the equation of the Darcy velocity (37). The scheme for (5) writes $\forall 1 \leq n \leq N_T$

$$\mathrm{div}^{\mathcal{T}}\left(\mathbf{U}_{\mathfrak{D}}^{n}\right) = q_{\mathcal{T}}^{+,n} - q_{\mathcal{T}}^{-,n}, \tag{36}$$

$$\mathbf{U}_{\mathfrak{D}}^{n} = -\frac{\mathbf{K}_{\mathcal{D}}(\nabla^{\widetilde{\mathfrak{D}}} p_{\mathcal{T}}^{n})}{\mu(c_{\mathfrak{D}}^{n-1})}, \tag{37}$$

$$\mathbf{U}_{\mathcal{D}}^{n} \cdot \mathbf{n} = 0, \quad \forall \mathcal{D} \in \mathfrak{D}_{ext}, \tag{38}$$

$$\sum_{\mathcal{K} \in \mathfrak{M}} \mathrm{m}_{\mathcal{K}} p_{\mathcal{K}}^{n} = \sum_{\mathcal{K}^* \in \overline{\mathfrak{M}^*}} \mathrm{m}_{\mathcal{K}^*} p_{\mathcal{K}^*}^{n} = 0, \tag{39}$$

and the scheme for (6) writes $\forall 1 \leq n \leq N_T$

$$\Phi_{\mathcal{T}} \frac{c_{\mathcal{T}}^{n} - c_{\mathcal{T}}^{n-1}}{\delta t} - \mathrm{div}^{\mathcal{T}}\left(\mathbb{D}_{\mathfrak{D}}\left(\mathbf{U}_{\mathfrak{D}}^{n}\right) \nabla^{\mathfrak{D}} c_{\mathcal{T}}^{n}\right) + \mathrm{divc}^{\mathcal{T}}\left(\mathbf{U}_{\mathfrak{D}}^{n}, c_{\mathcal{T}}^{n}\right) + q_{\mathcal{T}}^{-,n} c_{\mathcal{T}}^{n} = q_{\mathcal{T}}^{+,n} \hat{c}_{\mathcal{T}}^{n}, \tag{40}$$

$$\mathbb{D}_{\mathcal{D}}\left(\mathbf{U}_{\mathcal{D}}^{n}\right) \nabla^{\mathcal{D}} c_{\mathcal{T}}^{n} \cdot \mathbf{n} = 0, \forall \mathcal{D} \in \mathfrak{D}_{ext}. \tag{41}$$

5.4. Numerical experiments

Refinement level	DDFV		m-DDFV	
	error L^1	order L^1	error L^1	order L^1
1	1.63e-01	-	3.36e-02	-
2	7.95e-02	1.19	9.50e-03	2.10
3	3.83e-02	1.14	2.69e-03	1.97
4	1.78e-02	1.15	7.60e-04	1.90
5	7.64e-03	1.25	2.07e-04	1.92
6	2.55e-03	1.60	4.79e-05	2.13

Table 5.1: Test 1. Convergence results of the DDFV and m-DDFV on the pressure p at time $t = 3600$, with $\mathbb{K} = (80\mathbf{1}_{y<500} + 20\mathbf{1}_{y>500})\,\mathbb{I}$.

In this Section, we now illustrate the behavior of the m-DDFV scheme by applying it to the Peaceman model (1)–(3). We study the numerical rates of convergence of this scheme for the pressure and the concentration equations and we compare them to the numerical rates obtained with the DDFV-scheme.

We first consider the Test 1 introduced in Section 4 with a discontinuous permeability. As the viscosity is constant, this test case is an example where the pressure equation is decoupled from the concentration equation. In Table 5.1, we observe that the m-DDFV scheme has an order 2 of convergence for the pressure equation, while the DDFV-scheme

Refinement level	DDFV		m-DDFV	
	error L^1	order L^1	error L^1	order L^1
1	4.60e-02	-	4.76e-02	-
2	3.26e-02	0.57	3.31e-02	0.61
3	2.02e-02	0.75	2.04e-02	0.76
4	1.10e-02	0.92	1.10e-02	0.92
5	5.13e-03	1.12	5.17e-03	1.12
6	1.80e-03	1.53	1.81e-03	1.53

Table 5.2: Test 1. Convergence results of the DDFV and m-DDFV methods on the concentration c, at time $t = 3600$, with $\mathbb{K} = (80\mathbf{1}_{y<500} + 20\mathbf{1}_{y>500})\,\mathbb{I}$.

has only an order 1. However, we see in Table 5.2 that the values of the errors and the order of convergence obtained with the DDFV and the m-DDFV schemes are similar for the concentration equation: the order of convergence is around 1.

Then, we consider the Test 2 introduced in Section 4 with discontinuous permeability. In this test case, the viscosity is no more constant; it induces a strong coupling between the equations for the pressure and the concentration. We see in Tables 5.3 and 5.4 that the results obtained with the m-DDFV scheme are not really better than the results given by the DDFV-scheme. Indeed, the values of the error and of the order of convergence are similar for the concentration equation as for the pressure equation. It would be certainly valuable to use an higher order scheme for the concentration equation in order to keep the benefit of the use of a m-DDFV scheme for the pressure equation.

Refinement	DDFV		m-DDFV	
level	error L^1	order L^1	error L^1	order L^1
1	3.71e-01	-	2.50e-01	-
2	2.65e-01	0.56	2.10e-01	0.29
3	1.73e-01	0.66	1.60e-01	0.42
4	1.18e-01	0.57	1.14e-01	0.51
5	7.17e-02	0.74	7.03e-02	0.71
6	3.45e-02	1.07	3.41e-02	1.06

Table 5.3: Test 2. Convergence results of the DDFV and m-DDFV methods on the pressure p, at time $t = 3600$, with $\mathbb{K} = (80\mathbf{1}_{y<500} + 20\mathbf{1}_{y>500})\,\mathbb{I}$.

Refinement	DDFV		m-DDFV	
level	error L^1	order L^1	error L^1	order L^1
1	4.69e-01	-	4.70e-01	-
2	3.67e-01	0.41	3.71e-01	0.39
3	2.62e-01	0.53	2.64e-01	0.54
4	1.68e-01	0.67	1.68e-01	0.68
5	9.44e-02	0.85	9.45e-02	0.85
6	4.16e-02	1.20	4.16e-02	1.20

Table 5.4: Test 2. Convergence results of the DDFV and m-DDFV methods on the concentration c, at time $t = 3600$, with $\mathbb{K} = (80\mathbf{1}_{y<500} + 20\mathbf{1}_{y>500})\,\mathbb{I}$.

In order to compare the results given by the DDFV method and the Mixed Finite Volume Method presented in [9], we made numerical experiments on the same triangular mesh for Test 2 with the same time step. Figure 5.2 presents the level sets of the concentration obtained with both schemes at two different times (3 and 10 years). We observe that both schemes have the same qualitative behavior.

We finally introduce a last test case : **Test 3**. The only modification in Test 3 with respect to Test 2 is the value of the permeability. We consider here as in [9] the case where the permeability value is set to 80 except on four square subdomains where it is equal to 20. We compare the results given by the DDFV method and by the MFV method on a same squared mesh (with 25600 squares). Figure 5.3 shows the level sets of the concentration obtained with both schemes. We still observe that both schemes provide similar results.

In conclusion, we have presented a well-posed scheme for the Peaceman model, which is convergent and had good qualitative properties. From a qualitative point of view, our scheme gives similar results to the results obtained with the Mixed Finite Volume method. The proof of the convergence of the scheme will be achieved in a forthcoming paper.

[1] I. Aavatsmark, T. Barkve, O. Bøe, and T. Mannseth. Discretization on unstructured grids for inhomogeneous, anisotropic media. I. Derivation of the methods. *SIAM J. Sci. Comput.*, 19(5):1700–1716 (electronic), 1998.

[2] I. Aavatsmark, T. Barkve, O. Bøe, and T. Mannseth. Discretization on unstructured grids for inhomogeneous, anisotropic media. II. Discussion and numerical results. *SIAM J. Sci. Comput.*, 19(5):1717–1736 (electronic), 1998.

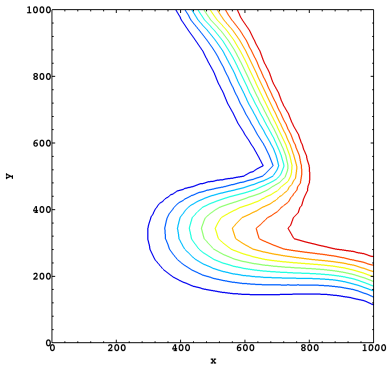

(a) DDFV scheme: concentration at time $t = 3$ years.

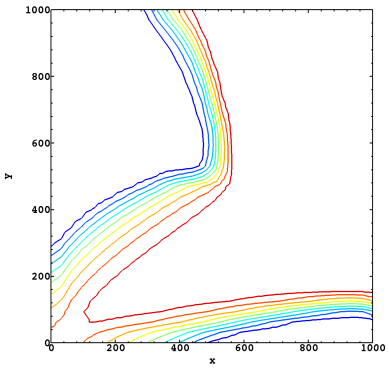

(b) DDFV scheme: concentration at time $t = 10$ years.

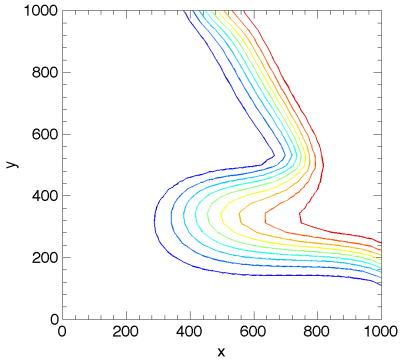

(c) MFV scheme: concentration at time $t = 3$ years.

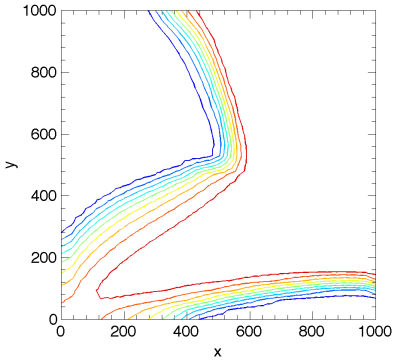

(d) MFV scheme: concentration at time $t = 10$ years.

Figure 5.2: Test2. Comparison of the results obtained with the DDFV and the MFV schemes: level sets of the concentration after 3 and 10 years.

[3] B. Amaziane and M. El Ossmani. Convergence analysis of an approximation to miscible fluid flows in porous media by combining mixed finite element and finite volume methods. *Numer. Methods Partial Differential Equations*, 24(3):799–832, 2008.

[4] B. Andreianov, M. Bendahmane, and K. H. Karlsen. Discrete duality finite volume schemes for doubly nonlinear degenerate hyperbolic-parabolic equations. *J. Hyperbolic Differ. Equ.*, 7(1):1–67, 2010.

[5] B. Andreianov, F. Boyer, and F. Hubert. Discrete duality finite volume schemes for Leray-Lions type elliptic problems on general 2D-meshes. *Num. Meth. for PDEs*, 23(1):145–195, 2007.

[6] J. Bear. *Dynamics of fluids in porous media*. American Elsevier, 1972.

[7] M. Bessemoulin-Chatard, C. Chainais-Hillairet, and F. Filbet. On discrete functional inequalities for some finite volume schemes. *submitted*, 2012.

[8] F. Boyer and F. Hubert. Finite volume method for 2d linear and nonlinear elliptic problems with discontinuities. *SIAM J. Numer. Anal.*, 46(6):3032–3070, 2008.

[9] C. Chainais-Hillairet and J. Droniou. Convergence analysis of a mixed finite volume scheme for an elliptic-parabolic system modeling miscible fluid flows in porous media. *SIAM J. Numer. Anal.*, 45(5):2228–2258 (electronic), 2007.

[10] Y. Coudière and G. Manzini. The discrete duality finite volume method for convection-diffusion problems. *SIAM J. Numer. Anal.*, 47(6):4163–4192, 2010.

[11] Y. Coudière, J.-P. Vila, and P. Villedieu. Convergence rate of a finite volume scheme for a two-dimensional convection-diffusion problem. *M2AN Math. Model. Numer. Anal.*, 33(3):493–516, 1999.

[12] Y. Coudière, J.-P. Vila, and P. Villedieu. Convergence rate of a finite volume scheme for a two-dimensional convection-diffusion problem. *M2AN Math. Model. Numer. Anal.*, 33(3):493–516, 1999.

[13] K. Domelevo and P. Omnes. A finite volume method for the Laplace equation on almost arbitrary two-dimensional grids. *M2AN Math. Model. Numer. Anal.*, 39(6):1203–1249, 2005.

[14] J. Douglas. *Numerical methods for the flow of miscible fluids in porous media.* John Wiley, 1984.

[15] J. Douglas, Jr., R. E. Ewing, and M. F. Wheeler. A time-discretization procedure for a mixed finite element approximation of miscible displacement in porous media. *RAIRO Anal. Numér.*, 17(3):249–265, 1983.

[16] J. Droniou. Finite volume schemes for fully non-linear elliptic equations in divergence form. *M2AN Math. Model. Numer. Anal.*, 40(6):1069–

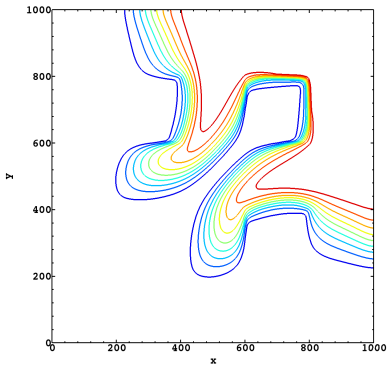

(a) DDFV scheme: concentration at time $t = 3$ years.

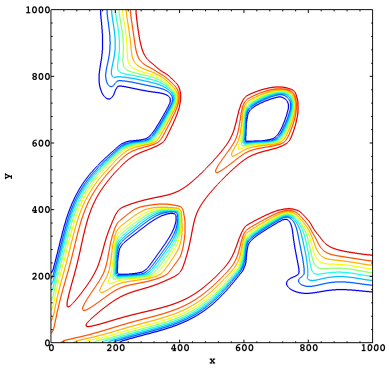

(b) DDFV scheme: concentration at time $t = 10$ years.

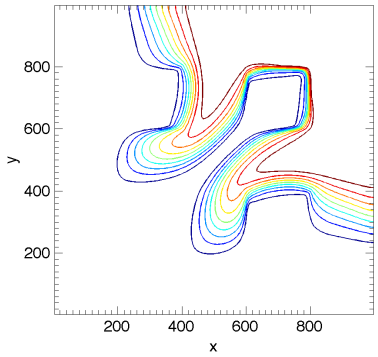

(c) MFV scheme: concentration at time $t = 3$ years.

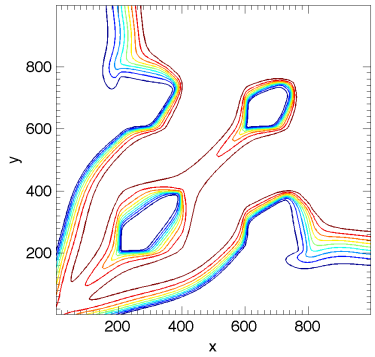

(d) MFV scheme: concentration at time $t = 10$ years.

Figure 5.3: Test3. Comparison of the results obtained with the DDFV and the MFV schemes: level sets of the concentration after 3 and 10 years.

1100 (2007), 2006.

[17] J. Droniou and R. Eymard. A mixed finite volume scheme for anisotropic diffusion problems on any grid. *Numer. Math.*, 105(1):35–71, 2006.

[18] R. E. Ewing, T. F. Russell, and M. F. Wheeler. Simulation of miscible displacement using mixed methods and a modified method of characteristics. *SPE*, 12241:71–81, 1983.

[19] R. E. Ewing, T. F. Russell, and M. F. Wheeler. Convergence analysis of an approximation of miscible displacement in porous media by mixed finite elements and a modified method of characteristics. *Comput. Methods Appl. Mech. Engrg.*, 47(1-2):73–92, 1984.

[20] R. Eymard, T. Gallouët, and R. Herbin. Finite volume methods. In Ph Ciarlet and J.L. Lions, editors, *Handbook of numerical analysis, Vol. VII*, Handb. Numer. Anal., VII, pages 715–1022. North-Holland, Amsterdam, 2000.

[21] R. Eymard, T. Gallouët, and R. Herbin. A new finite volume scheme for anisotropic diffusion problems on general grids: convergence analysis. *C. R. Math. Acad. Sci. Paris*, 344(6):403–406, 2007.

[22] R. Eymard, T. Gallouët, and R. Herbin. Discretization of heterogeneous and anisotropic diffusion problems on general nonconforming meshes SUSHI: a scheme using stabilization and hybrid interfaces. *IMA J. Numer. Anal.*, 30(4):1009–1043, 2010.

[23] R. Eymard, G. Henry, R. Herbin, F. Hubert, R. Klöfkorn, and G. Manzini. 3d benchmark on discretization schemes for anisotropic diffusion problems on general grids. In J. Fort, J. Fürst, J. Halama, R. Herbin, and F. Hubert, editors, *Proceedings of Finite Volumes for Complex Applications VI*, volume 2, pages 95–130. Springer, 2011.

[24] R. Herbin and F. Hubert. Benchmark on discretization schemes for anisotropic diffsion problems on general grids. In R. Eymard and J. M. Herard, editors, *Proceedings of Finite Volumes for Complex Applications V*, Aussois, France, 2008. Wiley.

[25] F. Hermeline. A finite volume method for the approximation of diffusion operators on distorted meshes. *J. Comput. Phys.*, 160(2):481–499, 2000.

[26] F. Hermeline. Approximation of diffusion operators with discontinuous tensor coefficients on distorted meshes. *Comput. Methods Appl. Mech. Engrg.*, 192(16-18):1939–1959, 2003.

[27] J. Jaffré and J. E. Roberts. Upstream weighting and mixed finite elements in the simulation of miscible displacements. *RAIRO Modél. Math. Anal. Numér.*, 19(3):443–460, 1985.

[28] A.-H. Le and P. Omnes. Discrete poincaré inequalities for arbitrary meshes in the discrete duality finite volume context. *submitted*, 2012.

[29] T. F. Russell. Finite elements with characteristics for two-component incompressible miscible displacement. In *Proceedings of 6th SPE*

symposium on Reservoir Simulation, pages 123–135, New Orleans, 1982.

[30] H. Wang, D. Liang, R. E. Ewing, S. L. Lyons, and G. Qin. An approximation to miscible fluid flows in porous media with point sources and sinks by an Eulerian-Lagrangian localized adjoint method and mixed finite element methods. *SIAM J. Sci. Comput.*, 22(2):561–581 (electronic), 2000.

[31] H. Wang, D. Liang, R. E. Ewing, S. L. Lyons, and G. Qin. An improved numerical simulator for different types of flows in porous media. *Numer. Methods Partial Differential Equations*, 19(3):343–362, 2003.